The American Journal of Pathology, Vol. 182, No. 5, May 2013

ELSEVIER

The American Journal of
PATHOLOGY
ajp.amjpathol.org

NEUROBIOLOGY

Blocking the Interaction between Apolipoprotein E and Aβ Reduces Intraneuronal Accumulation of Aβ and Inhibits Synaptic Degeneration

Magdalena A. Kuszczyk,* Sandrine Sanchez,* Joanna Pankiewicz,*† Jungsu Kim,‡§¶ Malgorzata Duszczyk,* Maitea Guridi,* Ayodeji A. Asuni,* Patrick M. Sullivan,‖** David M. Holtzman,‡§¶ and Martin J. Sadowski*†,††

From the Departments of Neurology, Biochemistry and Molecular Pharmacology,† and Psychiatry,†† New York University School of Medicine, New York, New York; the Department of Neurology,‡ the Knight Alzheimer's Disease Research Center,§ and the Hope Center for Neurological Disorders,¶ Washington University School of Medicine, St. Louis, Missouri; the Division of Geriatrics,‖ Department of Medicine, Duke University School of Medicine, Durham, North Carolina; and the Durham Veterans Health Administration Medical Center's Geriatric Research, Education and Clinical Center,** Durham, North Carolina*

Accepted for publication January 17, 2013.

Address correspondence to Martin J. Sadowski, M.D., Ph.D., New York University School of Medicine, 450E 29th St. ERSP, Rm. 830, New York, NY 10016. E-mail: sadowm01@med.nyu.edu.

Accumulation of β-amyloid (Aβ) in the brain is a key event in Alzheimer disease pathogenesis. Apolipoprotein (Apo) E is a lipid carrier protein secreted by astrocytes, which shows inherent affinity for Aβ and has been implicated in the receptor-mediated Aβ uptake by neurons. To characterize ApoE involvement in the intraneuronal Aβ accumulation and to investigate whether blocking the ApoE/Aβ interaction could reduce intraneuronal Aβ buildup, we used a noncontact neuronal-astrocytic co-culture system, where synthetic Aβ peptides were added into the media without or with cotreatment with Aβ12-28P, which is a nontoxic peptide antagonist of ApoE/Aβ binding. Compared with neurons cultured alone, intraneuronal Aβ content was significantly increased in neurons co-cultured with wild-type but not with ApoE knockout (KO) astrocytes. Neurons co-cultured with astrocytes also showed impaired intraneuronal degradation of Aβ, increased level of intraneuronal Aβ oligomers, and marked down-regulation of several synaptic proteins. Aβ12-28P treatment significantly reduced intraneuronal Aβ accumulation, including Aβ oligomer level, and inhibited loss of synaptic proteins. Furthermore, we showed significantly reduced intraneuronal Aβ accumulation in $APP_{SW}/PS1_{dE9}$/ApoE KO mice compared with $APP_{SW}/PS1_{dE9}$/ApoE targeted replacement mice that expressed various human ApoE isoforms. Data from our co-culture and *in vivo* experiments indicate an essential role of ApoE in the mechanism of intraneuronal Aβ accumulation and provide evidence that ApoE/Aβ binding antagonists can effectively prevent this process. *(Am J Pathol 2013, 182: 1750–1768; http://dx.doi.org/10.1016/j.ajpath.2013.01.034)*

Long-term accumulation of a toxic and insoluble β-amyloid (Aβ) peptide in the brain of patients with Alzheimer disease (AD) triggers a neurodegenerative cascade that involves widespread synaptic degeneration, formation of neurofibrillary tangles, and neuronal loss, which result in progressive dementia.[1,2] Buildup of Aβ is a result of a disequilibrium between the rate of its generation and the rate of its brain clearance[3] and is driven by inherently low solubility and natural propensity of Aβ to self-assemble into oligomers and fibrils.[4] Aβ fibrils, which are deposited as senile plaques and cerebral amyloid angiopathy (CAA), together with neurofibrillary tangles and synaptic degeneration, constitute neuropathologic hallmarks of AD. There is also evidence of intraneuronal Aβ accumulation in addition to the extracellular Aβ plaques and CAA, which may also contribute importantly to the Aβ-induced neurodegenerative cascade.[5–7]

A number of studies have associated intraneuronal Aβ buildup with hyperphosphorylation of tau protein,[8] disturbed protein trafficking and sorting,[9] reduced expression of synaptic proteins,[10] and mitochondrial dysfunction.[11,12]

Supported by grants from the NIH National Institute on Aging (R01 AG31221 and K02 AG34176 to M.J.S.; R37 AG13956 to D.M.H.) and by a Hartford/AFAR Beeson Scholars Collaborative Award (M.J.S. and D.M.H.).

http://dx.doi.org/10.1016/j.ajpath.2013.01.034

Apolipoprotein E (ApoE) is a 34-kDa lipid carrier protein with inherent affinity for Aβ, which is involved in multiple aspects of Aβ metabolism, including formation of Aβ plaques and CAA and impairment of Aβ brain clearance.[13] The pivotal role of ApoE in brain Aβ accumulation was confirmed by showing a marked reduction in Aβ plaque and CAA deposits associated with the *Apoe* gene knockout (KO) in AD transgenic (Tg) mice.[14] In the brain, ApoE is produced by astrocytes, which secrete ApoE-containing lipoprotein particles into the interstitial fluid from where they are internalized by neurons through receptor-mediated endocytosis. The propensity of ApoE to bind Aβ and its efficient internalization by neurons implicates ApoE in promoting neuronal Aβ uptake.[15] To characterize the role of ApoE in intraneuronal Aβ accumulation and to test the hypothesis that a therapeutic agent blocking the ApoE/Aβ binding could ameliorate intraneuronal Aβ buildup, we developed a noncontact, co-culture model that combined primary hippocampal neurons and astrocytes as a source of native, lipidated ApoE particles (Figure 1). The ApoE/Aβ binding was blocked with Aβ12-28P, which is a nontoxic, synthetic peptide modified for increased blood-brain-barrier (BBB) permeability and extended serum half-life.[16] As we have previously shown, Aβ12-28P inhibits ApoE4/Aβ binding with K_I = 12.9 nmol/L, neutralizes the promoting effect of ApoE on Aβ fibrillization *in vitro*, and reduces the load of Aβ plaques and CAA when systemically administered to APP_{SW} Tg mice.[22] In a complementary *in vivo* study included here, we analyzed the effect of ApoE KO and the effect of various human ApoE isoforms on the intraneuronal Aβ accumulation in newly developed APP_{SW}/$PS1_{dE9}$/ApoE KO and APP_{SW}/$PS1_{dE9}$/ApoE-TR (targeted replacement) mice. Our studies emphasize the pivotal role of ApoE in intraneuronal Aβ accumulation and show the benefits of pharmacologic targeting of the ApoE/Aβ interaction on intraneuronal Aβ levels and neurodegeneration.

Materials and Methods

Materials and Reagents

All Aβ peptides were custom synthesized in the WM Keck Proteomic Facility of Yale University (New Haven, CT). Unlabeled peptides were provided by the laboratory of Dr. James I. Elliott (Yale University), and fluorescein-tagged Aβ1-40 was synthesized by the laboratory of Dr. Janet Crawford (Yale University). PCR primers were custom synthesized by Gene Link (Hawthorne, NY). Recombinant human APOE4 was bought from Leinco Technologies, Inc. (St. Louis, MO). Cell culture plasticware, including Transwell inserts with 0.4-μm pore size, were purchased from Corning Incorporated (Corning, NY). Cell culture media and human aggregated Aβ enzyme-linked immunosorbent assay (ELISA) kit were purchased from Invitrogen Life Technologies (Carlsbad, CA). Complete Protease Inhibitor Cocktail was obtained from Roche Applied Science (Indianapolis, IN). A kit for bicinchoninic acid assay and the SuperSignal chemiluminescent reagent for immunoblotting were obtained from Pierce Biotechnology Inc. (Rockford, IL). Nitrocellulose membrane and horseradish peroxidase-conjugated secondary antibodies (Abs) for immunoblot analysis were sheep anti-mouse and donkey anti-rabbit (GE Healthcare Bio-Sciences Corp., Piscataway, NJ). Immobilon polyvinylidene difluoride membrane and Microcon centrifugal filter devices were purchased from Millipore Corporation (Billerica, MA). Autoradiography films X-Omat Blue XB-1 were bought from Eastman Kodak Company (New Haven, CT). Mouse on mouse (MOM) peroxidase kit, MOM blocking reagent, streptavidin/biotin blocking kit, and biotinylated secondary Abs included goat anti-mouse IgG and goat anti-rabbit IgG used for immunocytochemistry and immunohistochemistry (Vector Laboratories, Ltd., Burlingame, CA). All other reagents were purchased from Sigma-Aldrich (St. Louis, MO). Primary Abs were

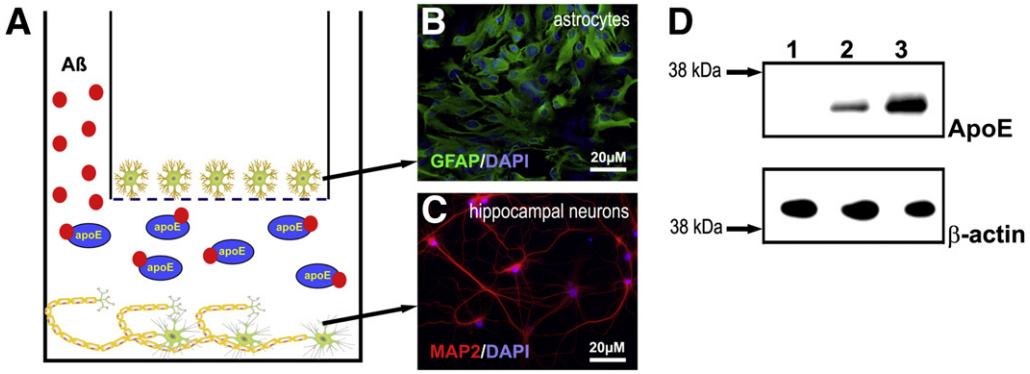

Figure 1 Noncontact, co-culture system of primary hippocampal neurons and astrocytes. **A:** Diagram of neuronal-astrocytic co-culture system. Astrocytes seeded on the Transwell insert are suspended above a monolayer of primary hippocampal neurons grown on the bottom of the well, whereas monomers of synthetic Aβ peptides are directly added into the conditioned media. **B:** Microphotograph of sentinel astrocytic cultures immunostained against GFAP and counterstained with DAPI. **C:** Microphotograph of sentinel primary hippocampal neuronal culture at seven DIV immunostained against neuronal cytoskeleton marker MAP2 and counterstained with DAPI. **D:** Western immunoblot analyses of murine ApoE and β-actin used as a loading control from lysates of primary hippocampal neurons cultured alone (**lane 1**), primary hippocampal neurons co-cultured with astrocytes (**lane 2**), and astrocytes cultured alone (**lane 3**). DIV, days *in vitro*; GFAP, glial fibrillary acidic protein; MAP2, microtubule-associated protein 2. Scale bars: 20 μM (**B** and **C**).

obtained from several different sources, and their listing, together with working dilutions, is provided in Table 1. HJ6.1 is a novel monoclonal antibody (mAb) against murine ApoE. It was generated with ApoE lipoprotein particles purified by affinity chromatography from media of primary astrocytic cultures established from C57BL/6 mice. Purified astrocyte-secreted ApoE lipoprotein particles were injected with complete Freund adjuvant to ApoE KO mice. For an initial screening of Abs, supernatant fluids from hybridoma cells (approximately 2000 wells) were added to 96-well plates coated with purified astrocyte-secreted ApoE lipoprotein particles. With the use of anti-mouse IgG-horseradish peroxidase as a detection antibody, we initially identified 36 clones and then subcloned them to find those that performed well in several biochemical and immunohistochemical assays.

Mice

All mouse care and experimental procedures were approved by Institutional Animal Care and Use Committees of the New York University School of Medicine and the Washington University School of Medicine. Cultures of primary hippocampal neurons and astrocytes were established from pups of C57BL/6 mice, whose breeding pairs were obtained from Charles River Laboratories (Wilmington, MA). Additional astrocytic cultures were established from ApoE KO mice described previously.[17] To develop the $APP_{SW}/PS1_{dE9}$/ApoE KO line, ApoE KO mice were doubled crossed with $APP_{SW}/PS1_{dE9}$ mice (line 85, stock number 004462; The Jackson Laboratory, Bar Harbor, ME). In $APP_{SW}/PS1_{dE9}$ mice, the mouse amyloid precursor protein (APP) harboring the human Aβ sequence with the double Swedish familial AD mutation K594M/N595L and human presenilin 1 (PS1) with exon 9 deletion (dE9) are expressed under the control of the mouse prion protein promoter and transmitted as a single Mendelian locus. $APP_{SW}/PS1_{dE9}$/ApoE KO founders were identified by PCR on MyiQ2 real-time PCR system (Bio-Rad, Hercules, CA) by using pairs of primers for *PS1* transgene (5′-TAAGTCAGTCAGCTTTTATACCCGGAAGGA-3′ and 5′-CAGGAGGATAGTCATGACAACAATGACACT-3′) and by showing lack of PCR product with *APOE* primers (5′-AGACGCGGGCACGGCTGT-3′ and 5′-CTCGCGGATGGCGCTGAG-3′). $APP_{SW}/PS1_{dE9}$/ApoE KO mice were then crossed back several times with ApoE-TR mice that carried one of the three human alleles (*APOE2*, *APOE3*, or *APOE4*) until the expression of $APP_{SW}/PS1_{dE9}$ transgene on the homozygote background of each of the three human ApoE isoforms was established. Each ApoE-TR mouse line contains mouse regulatory sequences and the noncoding murine exon 1 surrounding the inserted human exons 2′, 3′, and 4′.[18,19] Therefore, these mice express the human ApoE protein at physiological levels and retain the endogenous regulatory sequences required for modulating ApoE expression. $APP_{SW}/PS1_{dE9}$/ApoE-TR lines were maintained by breeding with ApoE isoform-matched ApoE-TR mice. Offspring were

Table 1 List of Antibodies Used in the Study

Antigen	Clone (symbol)	Type	Dilution IC/IH	Dilution WI/DI	Source
Aβ residues 1—16	6E10	Mouse monoclonal	1:1000	1:5000	Gift*
Aβ residues 17—24	4G8	Mouse monoclonal	1:1000	1:5000	Gift*
Aβ residues 1—16	HJ3.4	Mouse monoclonal	1:1000		Washington University in St. Louis, MO
Aβ40 C-terminus specific	HJ2	Mouse monoclonal		1:1000	Washington University in St. Louis
Aβ42 C-terminus specific	HJ7.4	Mouse monoclonal		1:2500	Washington University in St. Louis
Aβ oligomeric	A11	Rabbit polyclonal		1:500	Invitrogen
ApoE murine	HJ6.1	Mouse Monoclonal		1:1000	Washington University in St. Louis
APP N-terminus	22C11	Mouse monoclonal	1:1000		Millipore Corporation, Billerica, MA
APP C-terminus	A8717	Rabbit polyclonal	1:1000		Sigma-Aldrich
α-Tubulin	DM1A	Mouse monoclonal		1:2000	Sigma-Aldrich
β-Actin N-terminus	AC-15	Mouse monoclonal		1:1000	Sigma-Aldrich
Cathepsin D	H-75	Rabbit polyclonal	1:100		Santa Cruz Biotechnology, Santa Cruz, CA
EEA1	G-4	Mouse monoclonal	1:100		Santa Cruz Biotechnology
HSP60 residues 288—366	HSP60	Mouse monoclonal	1:100		Stressgen Bioreagents, Ann Arbor, MI
GFAP	3H2	Mouse monoclonal	1:1000		Sigma-Aldrich
GFAP	N1506	Rabbit polyclonal	1:2000		Dako North America Inc., Carpinteria, CA
MAP2	HM-2	Mouse monoclonal	1:1000		Sigma-Aldrich
NR1 subunit residues 834—938	NR-1, CT	Mouse monoclonal	1:100		Millipore Corporation
PSD-95	7E3-1B8	Mouse monoclonal	1:500		Millipore Corporation
Rab7	H-50	Rabbit polyclonal	1:100		Santa Cruz Biotechnology
Synaptophysin residues 221—313	H-8	Mouse monoclonal	1:200		Santa Cruz Biotechnology

*From Richard J. Kascsak (New York State Institute for Basic Research, Staten Island, NY).

APP, amyloid precursor protein; EEA1, early endosomal antigen 1; GFAP, glial fibrillary acidic protein; HSP60, heat shock protein 60; IC/IH-immunocytochemistry/immunohistochemistry; MAP2, microtubule-associated protein 2; PSD-95, postsynaptic density protein 95; WI/DI Western immunoblotting/dot immunoblotting.

identified by PCR. The human ApoE isoform status was verified by restriction fragment length polymorphism analysis of the human *APOE* gene PCR product.[20] Animals were bred and housed in a germ-free facility with 12/12-hour light/dark cycle and *ad libitum* food and water access. Given documented sex differences in Aβ deposition in the APP_{SW}/$PS1_{dE9}$ strain,[21] the load of Aβ plaques and intraneuronal Aβ accumulation were quantified only in female mice. All mice that were compared were on the same genetic background.

Handling of Synthetic Aβ Peptides

Aβ peptides were synthesized on solid-phase support and purified by reverse-phase high-pressure liquid chromatography, as previously described.[16,22] Full-length sequences of Aβ1-40, Aβ1-42, and Aβ1-40 amino-terminally tagged with 5,6-carboxyfluorescein (FITC-Aβ1-40) were synthesized with L-amino acids, whereas end-protected Aβ12-28P (NH_2-VHHQKLPFFAEDVGSNK-COOH) and its scrambled version $Aβ12\text{-}28P_S$ (NH_2-QGKFSDHVNEPHFAVKL-COOH) were synthesized with D-amino acids as previously described.[16,22] The purity of each batch of peptides was verified by mass spectrometry. Aβ peptides were treated with 1,1,1,3,3,3-hexafluoro-2-propanol (HFIP), which renders peptides monomeric with minimal β-sheet content,[4,16] and lyophilized. Lyophilized aliquots of Aβ peptides were stored at −80°C. Immediately before commencing cell culture experiments, Aβ peptides were directly reconstituted in cell culture media to achieve the concentration used in particular experiments.

Aβ oligomers were prepared according to established protocols[4,23,24] by incubating 100 μmol/L Aβ1-42 in serum and phenol-free Dulbecco's modified Eagle's medium mixed 1:1 with Ham's F12 medium, then centrifuged with Microcon YM-10 concentrators to remove unaggregated Aβ monomers.

Cell Culture Preparation

Cultures of primary hippocampal neurons and astrocytes were established from pups within 24 hours from birth (P0 to P1). Animals were sacrificed by decapitation, and their brains were immediately removed from skulls in aseptic conditions. To establish cultures of primary hippocampal neurons, the hippocampi were dissected from both hemispheres under AmScope stereoscopic microscope (AmScope, Chino, CA). Fragments of hippocampal tissue were placed in the ice-cold Hank's balanced salt solution free of Ca^{2+} and Mg^{2+} and gently cut further into fine pieces that were then treated with 0.05% trypsin in Hank's balanced salt solution for 10 minutes at 37°C to obtain cell suspension. After the addition of 0.1% type-I-S trypsin inhibitor and 0.05% DNase I, the cell suspension was centrifuged at 500 × *g* for 30 seconds. The resulting pellet was triturated, centrifuged again at 500 × *g* for 5 minutes, and resuspended in the minimal essential medium (MEM) supplemented with heat-inactivated 10% fetal bovine serum (FBS), 0.5 mmol/L glutamine, 50 μg/mL streptomycin, and 50 U/mL penicillin. Cell suspension was then filtered through a 70-μm mesh, and the neurons were manually counted with the use of a hemotocytometer (Hausser Scientific, Horsham, PA) and seeded on poly-L-lysine–coated 12-well plates. For biochemical analysis, 5×10^5 neurons were seeded directly on the bottom of each well, whereas, for immunohistochemistry, removable poly-L-lysine–coated round coverslips were placed on the bottom of the wells, and the number of seeded neurons was reduced to 1×10^5 per well. The neurons were allowed to adhere to the surface for 4 hours, and then the medium was replaced with the serum-free Neurobasal medium containing 2% B27 supplement, 0.5 mmol/L glutamine, 50 μg/mL streptomycin, and 50 U/mL penicillin. At 3 days *in vitro* (DIV), 5 μmol/L cytosine-β-D-arabinoside was added to inhibit division of nonneuronal cells. The neurons were fed by replacing one-third of the medium volume every 72 hours. At 7 DIV, one well from each preparation of primary hippocampal neurons was randomly selected to determine the purity of the culture and was immunostained against a neuronal-specific marker, the microtubule-associated protein 2 (MAP2), followed by nucleic acid stain DAPI (Figure 1C). The ratio of MAP2-positive to DAPI-positive cells was then calculated to assess culture purity. Those cultures that showed a purity of at least 90% were grown further until 14 DIV when neurons reach their mature form and express functional glutamatergic receptors.[25]

Cultures of astrocytes were established from the brain cortex according to the protocol of Leroux et al.[26] After stripping the brain from the meninges and visible brain vessels, the cortical mantle was separated from the white matter and subcortical structures and gently cut into fine pieces in ice-cold Hank's balanced salt solution free of Ca^{2+} and Mg^{2+}. Cell suspension was prepared by gentle trituration of cortical tissue and then centrifuged for 5 minutes at 500 × *g*. The pellet was resuspended in MEM supplemented with 20% FBS, 2 mmol/L glutamine, 50 μg/mL streptomycin, and 50 U/mL penicillin, and the cells were introduced to 25-cm^2 flasks. Two days after establishing the astrocytic culture, a single dose of 5 μmol/L cytosine-β-D-arabinoside was added. After 6 days of growth, the FBS content in MEM was decreased to 10%, and astrocytes were grown until confluence. To determine the purity of the astrocytic cultures, the cells were seeded on a coverslip, fixed with methanol, and immunostained against glial fibrillary acidic protein and counterstained with DAPI. Cultures containing 90% or more glial fibrillary acidic protein-positive astrocytes were used for co-culture experiments (Figure 1B). Production of ApoE by astrocytes was confirmed with Western immunoblot analysis with HJ6.1 mAb against murine ApoE in astrocytic lysates and media (Figure 1D).

To set up the neuronal-astrocytic co-culture system, astrocytes were harvested with the use of 0.25% trypsin and 0.03% EDTA, suspended in MEM with 10% FBS, and counted with the use of a hemocytometer. Astrocytes were then plated on the top side of the poly-L-lysine–coated polycarbonate membranes of the Transwell inserts[27] (2×10^4 per insert) and cultured in MEM supplemented by 10% FBS,

2 mmol/L glutamine, 50 μg/mL streptomycin, and 50 U/mL penicillin for 48 hours followed by serum-free Neurobasal medium supplemented with 2% B27 and 0.5 mmol/L glutamine for 24 hours before combining the cultures. Transwell inserts with attached astrocytes were transferred into 12-well plates and positioned 2 mm above the neuronal monolayer growing on the bottom of the well (Figure 1A). Pores in the polycarbonate membranes of the Transwell insert allow for free passage of astrocyte-derived molecules, including lipidated ApoE complexes. The co-culture was maintained together in serum-free Neurobasal medium supplemented with 2% B27, 0.5 mmol/L glutamine, 50 μg/mL streptomycin, and 50 U/mL penicillin for 24 hours before commencing experiments. The astrocytes were always combined with neurons when neurons were 14 DIV, and the co-culture experiments were commenced when neurons were 15 DIV. The ApoE uptake by the primary hippocampal neurons was confirmed by Western immunoblot detection of ApoE in lysates from neurons co-cultured with astrocytes, whereas in the lysates of primary hippocampal neurons grown as a monoculture the ApoE signal was absent (Figure 1D).

Treatments of Neuronal Monocultures and Co-Culture Systems with Aβ Peptides

Monomerized Aβ1-40 and Aβ1-42 peptides were diluted with the Neurobasal medium to 10 μmol/L final concentration and added without or with 10 μmol/L Aβ12-28P or a control peptide Aβ12-28P$_S$ to neuronal-astrocytic co-cultures or neuronal monocultures for 24 or 72 hours. In confocal microscopy experiments designed to directly visualize intraneuronal Aβ accumulation, Aβ1-40 was traced with 10% FITC-Aβ1-40. In the experiment designed to investigate the effect of ApoE on intraneuronal degradation of internalized Aβ, 10 μmol/L Aβ1-40 was added to the medium for 6 hours, and then the cells were further grown in the Aβ-free medium during the 48-hour washout period. At the conclusion of each experiment, co-cultures were disassembled by removing Transwell inserts with attached astrocytes, and the primary hippocampal neurons grown on the bottom of the well were subjected to lysis or fixation for biochemical or immunohistochemical analyses, respectively. Each treatment experiment in neuronal-astrocytic co-cultures or neuronal monocultures was repeated three to six times.

Western Blot and Dot Immunoblot Analysis

Primary hippocampal neurons were washed three times with PBS at 37°C and gently treated with 0.1% trypsin and 0.03% ethylenediaminetetraacetic acid in PBS to remove remnants of noninternalized Aβ attached to their external surfaces.[28] Neurons were then harvested with ice-cold lysis buffer that contained 50 mmol/L Tris-HCl, pH 7.4, 150 mmol/L NaCl, 1 mmol/L ethylenediaminetetraacetic acid, 1% Nonidet-P40, 0.1% SDS, 0.2% diethylamine, 1 mmol/L phenylmethylsulfonyl fluoride, 10 μg/mL Complete Protease Inhibitor Cocktail supplemented with leupeptin, antipain, and pepstatin (5 μg/mL each).[22] The lysates were collected into 2-mL low-adhesion tubes, further homogenized with 10 strokes of a Teflon pestle, and centrifuged at 10,000 × *g* for 20 minutes at 4°C. The pellets containing cell debris were discarded, and the total protein concentration in the supernatant fluid was determined with the bicinchoninic acid assay. Samples of cell lysates that contained equal amounts of total protein were titrated with reducing Laemmli buffer to achieve equal volumes, boiled for 5 minutes, and then subjected to SDS-PAGE with the use of 15% gels. Under aforedescribed reducing conditions, most Aβ contained in the cell lysates appeared as monomers and dimers at the bottom of the membrane, which facilitated its densitometric quantification (Supplemental Figure S1, A and B). After Western blot transfer, nitrocellulose membranes were immunoblotted with 1:1 mixture of 6E10 and 4G8 mAbs[29] followed by horseradish peroxidase-conjugated sheep anti-mouse secondary Ab in 1:3000 dilution and the application of SuperSignal chemiluminescent reagent. To assure that Aβ12-28P, which has sequence overlap with the 4G8 epitope, does not alter 4G8 signal, a control experiment was conducted whereby synthetic Aβ1-40 or Aβ1-42 peptides were loaded on the gel alone or premixed with Aβ12-28P, and the membranes were immunoblotted with the 6E10/4G8 mixture, 6E10, and 4G8 alone, and mAbs HJ2 and HJ7.4, which are specific for C-termini of Aβ$_{X\text{-}40}$ and Aβ$_{X\text{-}42}$ peptides,[30] respectively (Supplemental Figure S2A). There was no evidence that Aβ12-28P changes detectability of Aβ1-40 or Aβ1-42 × 6E10 and 4G8, whereas Aβ12-28P alone was unrecognized by these mAbs. Furthermore, selected membranes that represented various treatment conditions were stripped and reprobed with Aβ C-terminal−specific mAbs that obtained a pattern of immunostaining comparable with that of the 6E10/4G8 mixture (Supplemental Figure S2B).

For detection of ApoE in lysates of primary hippocampal neurons and astrocytes and in the conditioned media, the samples were subjected to 10% SDS-PAGE under reducing conditions, and the membranes underwent immunoblot analysis with HJ6.1 mAb. For dot blot detection of Aβ oligomers, samples of neuronal lysates that contained equal amounts of total protein were titrated with PBS to achieve equal volumes of 20 μL and were blotted under vacuum onto polyvinylidene difluoride membranes. The membranes were immunoblotted with A11 oligomer-specific polyclonal Ab.[31] Samples that contained preparations of HFIP monomerized Aβ1-42 and *in vitro* oligomerized Aβ1-42 were used as negative and positive controls, respectively. Lysates from 15-DIV primary hippocampal neurons cultured in the absence of Aβ peptides, astrocytes, and human recombinant ApoE4 were used as additional controls (Supplemental Figure S2C).

Densitometric Analysis of Immunoblots

Autoradiography films were converted into 8-bit grayscale digital files with the use of a Epson Perfection 4990 scanner (Epson America, Long Beach, CA) and Adobe Photoshop version CS4 (Adobe Systems, San Jose, CA) and saved in

a TIFF format with a resolution of 600 dpi. Densitometric analysis of Aβ Western and dot blot signals was performed with NIH Image J software version 1.42 (Bethesda, MD) as previously described.[32,33]

Quantification of Aβ Oligomers by ELISA

Samples of neuronal lysates that contained 15 μg of total protein were titrated with PBS to achieve equal volumes. Concentration of Aβ oligomers in the lysate samples was determined with Human Aggregated β-Amyloid ELISA Kit, following the manufacturer-provided manual. After background subtraction, absorbance values from serially diluted samples of aggregated Aβ provided by the manufacturer as a part of the ELISA kit were used to generate a standard curve in GraphPad Prism version 5.02 (GraphPad Software, Inc., San Diego, CA) with the use of a nonlinear curve-fitting algorithm. Concentration of Aβ oligomers in samples of neuronal lysates was determined by comparing their absorbance values against the standard curve and were given in nanograms per milligram of the total protein in the lysate.

Immunocytochemistry and Quantification of Synaptic Protein Expression

Coverslips with attached primary hippocampal neurons were immersed three times in PBS at 37°C, then in 80% ice-cold methanol for 10 minutes to fix the neurons, and washed again three times in PBS. Nonspecific bindings of the primary Abs and streptavidin were blocked with MOM blocking mixture for 1 hour, followed by the streptavidin/biotin blocking kit for 30 minutes. Intraneuronal organelles were identified with a panel of Abs against organelle-specific markers: MAP2 for the cytoskeleton, early endosomal antigen 1 for early endosomes, Rab7 for late endosomes, Cathepsin D for late endosomes and lysosomes, and heat shock protein 60 for mitochondria (Table 1). Synaptic proteins specific for excitatory glutamatergic synapses of primary hippocampal neurons, including the NR1 subunit of the *N*-methyl-D-aspartic acid receptor (NMDAR), post-synaptic density protein 95 (PSD-95), which is functionally and structurally associated with NMDARs, and a major synaptic vesicle protein synaptophysin were immunodetected with the use of specific mAbs listed in Table 1. We used 1:1000 biotinylated secondary Abs followed by 1:500 cyanine 3-conjugated streptavidin to detect binding of primary Abs to their antigens. Neuronal nuclei were counterstained with DAPI. Immunostained neurons were analyzed with an 80i Nikon fluorescent microscope (Nikon Corp., Tokyo, Japan). Negative controls for immunocytochemistry included primary hippocampal neurons immunostained with anti-rabbit and anti-mouse biotinylated secondary antibodies with omission of the primary antibodies (Supplemental Figure S3A) and astrocytic cultures immunostained with mAbs for NR1, PSD-95, and synaptophysin (Supplemental Figure S3B).

To determine the expression of the synaptic proteins, at least 20 neurons from each treatment group per experiment from three independent experiments were photographed with the use of ×100 immersion oil objective. The images were captured with a high-sensitivity, cooled, monochrome DS-Qi1Mc camera and NIS Elements Imaging Software version 3.01 (Nikon Corp.) and saved in a TIFF format with a resolution of 600 dpi. With the use of NIH ImageJ software version 1.42, five rectangular test areas that measured 20 × 4 μmol/L each were randomly superimposed along the primary and secondary dendrites of each examined neuron, with the long axis of the test area oriented parallel to the long axis of the dendrites. Synaptic densities within the test area were automatically thresholded and filtered according to the preset algorithm to discriminate nonspecific staining. Data were expressed as the percentage values, using as 100% the average from the total area of synaptic protein puncta per test field in DIV-matched control primary hippocampal neurons.

Subcellular localization of internalized Aβ was examined by two- or three-channel confocal microscopy. Serial Z stacks of 0.5 μm thick tomograms were collected simultaneously in fluorescein and rhodamine channels with the use of a Bio-Rad Radiance 2000 confocal system mounted on the Olympus BX50WI fluorescence microscope (Olympus America Inc., Center Valley, PA). Zeiss LSM 510 confocal microscope (Carl Zeiss Microscopy GmbH, Jena, Germany) was used to collect Z stacks of 0.2 μm thick tomograms in fluorescein, rhodamine, and Texas Red channels. Captured stacks of images were further analyzed with Zeiss LSM Image Browser software version 4.2.0.121 or NIH ImageJ software version 1.42.

Histology, Immunohistochemistry, and Quantitative Analysis of Aβ Plaque Load and Intraneuronal Aβ Accumulation in $APP_{SW}/PS1_{dE9}$/ApoE KO and $APP_{SW}/PS1_{dE9}$/ApoE-TR Tg Mice

Eleven-month-old female Tg mice were sacrificed with an intraperitoneal injection of 150 mg/kg sodium pentobarbital and transcardially perfused with heparinized PBS. Brains were fixed by immersion in 4% paraformaldehyde in 0.1 phosphate buffer, pH 7.4, for 48 hours. Brains were dehydrated in a mixture of 20% glycerol and 20% dimethyl sulfoxide in PBS for 72 hours and cut into 40-μm–thick coronal sections on a freezing microtome. Serial sections were collected in 10 separate series, each containing every tenth section cut along the rostrocaudal brain axis. Randomly selected series were stained with thioflavine-S,[22] and X-34 dye[21] for fibrillar Aβ deposits and immunostained with HJ3.4 monoclonal Ab,[21] followed by MOM peroxidase kit to visualize the full spectrum of extracellular Aβ deposits containing its fibrillar and nonfibrillar forms. Negative controls for HJ3.4 immunohistochemistry included sections from C57BL/6 mice and sections from $APP_{SW}/PS1_{dE9}$/

ApoE4 mice immunostained with omission of HJ3.4 (Supplemental Figure S3C). The Aβ plaque load in the neocortex (percentage of cross-sectional area covered by Aβ) was quantified on X-34-stained sections in a blinded manner according to unbiased stereologic principles (Cavalieri-point counting method) as previously published.[21]

For the analysis and quantification of intraneuronal Aβ accumulation, brains were embedded in paraffin and cut into 10-μm−thick coronal sections, which were mounted on glass slides. After deparaffinization, sections were washed three times in PBS, and nonspecific bindings of the primary Abs and streptavidin were blocked with MOM blocking mixture for 1 hour, followed by the avidin/biotin blocking kit for 30 minutes. 6E10/4G8 mAb mixture was then added for 2 hours followed by 1:1000 biotinylated goat anti-mouse IgG secondary Ab for 1 hour and 1:500 FITC-conjugated streptavidin for 30 minutes. MOM blocking mixture was applied again for 1 hour, followed by anti-MAP2 Ab and cyanine 3-conjugated sheep anti-mouse secondary Ab. Vigorous washing was performed between each step of double immunofluorescence staining. The sections were analyzed under Bio-Rad Radiance 2000 confocal system mounted on the Olympus BX50WI fluorescence microscope. Ten stacks of confocal images spanning the entire thickness of the pyramidal layer of the CA1 and CA2/3 cornu ammonis sectors per section were taken from five to seven serial sections per brain. Neurons positive for intraneuronal $A\beta_{1\text{-}X}$ were identified only as those which were displaying bright punctuate immunostaining pattern inside the perikaryon, but not those showing weak, diffuse membrane staining. The number of neurons positive for intraneuronal $A\beta_{1\text{-}X}$ against the total number of neurons visualized by anti-MAP2 neuronal cytoskeletal staining was quantified and averaged per hippocampal sector in a given mouse brain. Additional hippocampal sections were immunostained with antibodies against C-terminus of $A\beta_{X\text{-}42}$, and amino and carboxy termini of APP, followed by DAPI counterstaining to control for the specificity of 6E10/4G8 immunostaining and the effect of ApoE KO on APP expression. Negative control for immunohistochemistry included hippocampal sections from C57BL/6 mice immunostained with anti-Aβ and anti-APP Abs (Supplemental Figure S3D).

Statistical Analysis

The statistical analysis was performed with GraphPad Prism version 5.02 (GraphPad Software, Inc.). Differences in the levels of the intraneuronal Aβ and expression of synaptic proteins were analyzed using repeated measures one-way analysis of variance followed by the Tukey's HSD post hoc test. Two-way analysis of variance followed by Bonferroni's post hoc test was used to analyze differences in the number of hippocampal neurons with intraneuronal Aβ deposits between CA1 and CA2/3 hippocampal sectors and between APP_{SW}/PS_{dE9}/ApoE KO and various APP_{SW}/PS_{dE9}/ApoE-TR lines. The *U*-test was used to analyze the therapeutic effect of Aβ12-28P in co-culture system on the intraneuronal Aβ oligomer level and differences in the load fibrillar Aβ deposits between various $APP_{SW}PS1_{dE9}$/ApoE-TR lines.

Results

Primary Hippocampal Neurons Co-Cultured with Astrocytes Show Increased Intraneuronal Accumulation of Aβ Peptides, Which Can Be Reduced with the ApoE/Aβ Binding Antagonist Aβ12-28P

Uptake of Aβ1-40 and Aβ1-42 from the conditioned media and their intraneuronal accumulation was compared between the primary hippocampal neurons cultured alone and the primary hippocampal neurons co-cultured with astrocytes combined in a noncontact neuronal-astrocytic co-culture system (Figure 1). In this *in vitro* experimental system, synthetic Aβ1-40 or Aβ1-42 peptides monomerized by HFIP treatment were added to the culture media once at the commencement of the experiment in the final concentration of 10 μmol/L. Both the primary hippocampal neurons and astrocytes (unless specifically stated otherwise) were derived from C57BL/6 wild-type mice. We also confirmed that neurons co-cultured with astrocytes internalize ApoE secreted by astrocytes to the conditioned media. This was done by Western immunoblot detection of ApoE in lysates of neurons co-cultured with astrocytes, whereas in the lysates of neurons cultured alone the ApoE signal was absent (Figure 1D).

Shown in Figure 2, A and B, are comparisons of intraneuronal levels of Aβ1-40 and Aβ1-42 between primary hippocampal neurons cultured alone or co-cultured with astrocytes for 24 hours in the presence of Aβ1-40 and Aβ1-42 peptides, respectively. Although the primary hippocampal neurons cultured alone showed internalization of Aβ1-40 and Aβ1-42 peptides from the media, the intraneuronal accumulation of both Aβ peptides was significantly increased in neurons, co-cultured with astrocytes. The intraneuronal level of Aβ1-40 in neurons from neuronal-astrocytic co-cultures was at 150.8% ± 3.6% (means ± SEM) of the level of neurons cultured alone ($P < 0.001$) (Figure 2A and Supplemental Figure S1A), whereas the level of Aβ1-42 was at 227.1% ± 26.4% of the level of neurons grown alone ($P < 0.01$) (Figure 2B and Supplemental Figures S1B and S2B). When Aβ12-28P, the antagonist of the ApoE/Aβ interaction, was added to the culture media together with Aβ1-40 and Aβ1-42 at the commencement of the experiment (10 μmol/L final concentration), intraneuronal levels of Aβ1-40 and Aβ1-42 peptides were reduced to 46.6% ± 4.8% ($P < 0.001$) and 82.8% ± 9.0%, respectively ($P < 0.01$), of those in neurons cultured alone. $A\beta12\text{-}28P_S$, a control peptide that represents a scrambled sequence of Aβ12-28P, had no significant effect on intraneuronal levels of Aβ1-40 and Aβ1-42 peptides in primary hippocampal neurons co-cultured with astrocytes. Moreover, Aβ12-28P had no effect on the

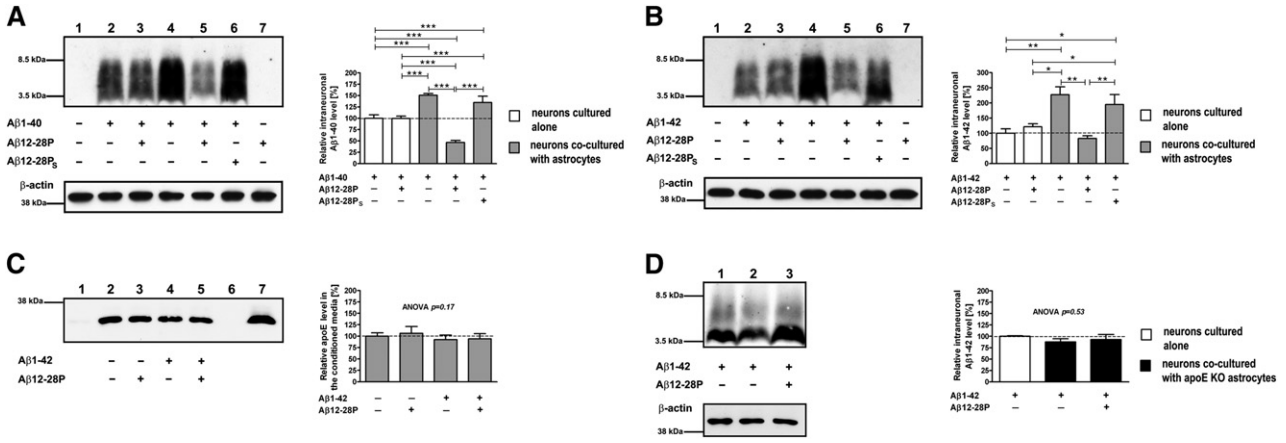

Figure 2 Western immunoblot analysis of the intraneuronal Aβ1-40 and Aβ1-42 content. **A** and **B**: Representative immunoblots for Aβ1-40 and Aβ1-42 in lysates of primary hippocampal neurons, respectively. Lanes 1, 2, 3 and 7 represent primary hippocampal neurons cultured alone, whereas lanes 4, 5, and 6 represent primary hippocampal neurons co-cultured with astrocytes. Exposure to Aβ1-40 and Aβ1-42 and cotreatment with Aβ12-28P and Aβ12-28P$_S$ are indicated directly underneath each lane. Samples containing 10 μg and 5 μg of total protein per lane were loaded in A and B, respectively. The full Western immunoblot analyses are provided in Supplemental Figure S1. Included are also Western immunoblot analyses for β-actin, which was used as a loading control. Values in the graphs show the mean percentage ± SEM of Aβ1-40 and Aβ1-42 band optic densities relative to those in neurons cultured alone during exposure to Aβ peptides (lane 2) in five and four independent experiments that used Aβ1-40 (analysis of variance $P < 0.0001$) and Aβ1-42 (analysis of variance $P = 0.0006$), respectively. Values of post hoc pair analysis obtained with Tukey's HSD test are displayed on the graph if statistically significant. **C**: Western immunoblot analysis for ApoE in the conditioned media of neuronal-astrocytic co-cultures under various Aβ1-42 and Aβ12-28P treatment conditions (lanes 2–5). Samples of the conditioned media from primary hippocampal neurons cultured alone (lane 1) and high-density astrocytic monoculture grown in the cell culture flask (lane 7) are shown as a negative and a positive control, respectively. Lane 6 was intentionally left unloaded. Values in the graph show the mean percentage ± SEM of ApoE band optic densities relative to those in neuronal-astrocytic co-cultures maintained without addition of any Aβ peptides in three independent experiments (analysis of variance $P = 0.17$). **D**: Immunoblot for Aβ1-42 in lysates of primary hippocampal neurons cultured alone (lane 1) and primary hippocampal neurons co-cultured with ApoE KO astrocytes without or with cotreatment with Aβ12-28P (lanes 2 and 3, respectively). Included is also Western immunoblot analyses for β-actin, which was used as a loading control. Values in the graph show the mean percentage ± SEM of Aβ1-42 band optic densities relative to those in neurons cultured alone during exposure to Aβ1-42 in three independent experiments (analysis of variance $P = 0.53$). $^*P < 0.05$, $^{**}P < 0.01$, and $^{***}P < 0.001$.

intraneuronal level of Aβ peptides, when it was added to primary hippocampal neurons cultured alone in the presence of Aβ1-40 or Aβ1-42 peptides. No significant differences were observed in the ApoE level in the conditioned media among various experimental conditions, which could account for the differences in the intraneuronal levels of Aβ peptides (Figure 2C).

To confirm that the increased intraneuronal accumulation of Aβ peptides in neurons co-cultured with astrocytes was directly related to astrocyte-secreted ApoE, we conducted a control experiment in which neuronal-astrocytic co-cultures were set up from primary hippocampal neurons derived from C57BL/6 wild-type mice and astrocytes derived from ApoE KO mice, which were on the C57BL/6 background. Concentrations and length of exposure to Aβ1-42 and Aβ12-28P were exactly matching the conditions in experiments with neuronal-astrocytic co-cultures that used wild-type astrocytes. No statistically significant differences in the intraneuronal Aβ1-42 level were appreciated between primary hippocampal neurons cultured alone and those co-cultured with ApoE KO astrocytes. Aβ1-42 level in neurons co-cultured with ApoE KO astrocytes was at 87.8% ± 6.8% of the Aβ1-42 level of neurons cultured alone, whereas, in neurons co-cultured with astrocytes and additionally treated with Aβ12-28P, the intraneuronal Aβ1-42 level was at 93.0% ± 10.9% of the Aβ1-42 level of neurons cultured alone (differences statistically not significant) (Figure 2D).

Furthermore, we investigated whether co-culturing of neurons with astrocytes affected intraneuronal level of Aβ oligomeric assemblies as well as the rate of intraneuronal degradation of internalized Aβ. Two independent methods were used to characterize intraneuronal content of Aβ oligomers, namely a dot immunoblot analysis that used A11 oligomer-specific Ab and ELISA specific for human-aggregated Aβ. We saw 11.8- and 1.7-fold increase ($P < 0.001$) in the level of intraneuronal Aβ1-40 and Aβ1-42 oligomers in primary hippocampal neurons co-cultured with astrocytes compared with those cultured alone, respectively (Figure 3A). Note that the primary hippocampal neurons cultured alone showed an approximately sevenfold greater level of intraneuronal Aβ1-42 oligomers than Aβ1-40 oligomers ($P < 0.001$), whereas no statistically significant difference between Aβ1-42 and Aβ1-40 oligomer levels was noted in neurons co-cultured with astrocytes. This observation indicated that ApoE more effectively promotes oligomerization of Aβ1-40, which has weaker self-aggregation properties than Aβ1-42, which is inherently more prone to form oligomers. The treatment of primary hippocampal neurons co-cultured with astrocytes with Aβ12-28P, which was added to the culture media together with Aβ1-40 and Aβ1-42 at the commencement of the experiment, produced a significant reduction in the intraneuronal Aβ oligomer level. The concentration of intraneuronal Aβ1-40 oligomers in neurons from untreated

co-cultures was 57.5 ± 8.3 ng/mg, whereas under Aβ12-28P treatment it was reduced to 30.0 ± 6.3 ng/mg ($P < 0.05$) as determined by ELISA specific for aggregated Aβ. The concentration of Aβ1-42 oligomers was 57.5 ± 5.9 ng/mg, whereas under Aβ12-28P treatment it was reduced to 40.0 ± 6.3 ng/mg ($P < 0.05$) (Figure 3B).

The effect of ApoE on the intraneuronal degradation of internalized Aβ was investigated by comparing how effectively primary hippocampal neurons cultured alone and those co-cultured with astrocytes degraded Aβ1-40 internalized during time-limited exposure (Figure 4, A and B). Neuronal monocultures and neuronal-astrocytic co-cultures were exposed to monomerized, synthetic Aβ1-40 peptide for 6 hours (10 μmol/L final concentration in the conditioned media at the commencement of the experiment), then the conditioned media were replaced with Aβ1-40–free media, and neurons were grown further in monoculture or in co-culture with astrocytes (washout period). Primary hippocampal neuron culture alone degraded 50% of the internalized Aβ1-40 within 3.2 hours, and no Aβ1-40 was detectable in their lysates at 24 hours after the commencement of the washout period. In contrast, the primary hippocampal neurons co-cultured with astrocytes still showed the presence of intraneuronal Aβ1-40 at 24 and 48 hours after the commencement of the washout period, which was 43.7% ± 4.9% and 32.9% ± 9.2%, respectively, of the Aβ1-40 signal at t = 0 hours.

We also analyzed the levels of Aβ1-40 and Aβ1-42 peptides in the conditioned media of the primary hippocampal neurons cultured alone and in the conditioned media of neuronal-astrocytic co-cultures (Supplemental Figure S4, A and B). We noted that at the conclusion of the experiment, a significant reduction was seen in the levels of both Aβ1-40 and Aβ1-42 peptides in the conditioned media from neuronal-astrocytic co-cultures compared with the levels of Aβ peptides in the conditioned media from neuronal monocultures. This effect was likely caused by the active clearance of Aβ peptides from the media by astrocytes. To confirm that astrocytes can robustly clear Aβ peptides from the conditioned media, we conducted a complementary experiment in which monomerized, synthetic Aβ1-40 or Aβ1-42 peptides were added to the media of astrocytes cultured alone (10 μmol/L final concentration at t = 0 hours), and then changes in the level of Aβ peptides in the media were analyzed over time. At t = 24 hours levels of Aβ1-40 and Aβ1-42 were reduced by 30.8% ± 6.3% and 24.4% ± 4.9%, respectively, compared with the levels of Aβ peptides at t = 0 hours, whereas at t = 96 hours levels of Aβ1-40 and Aβ1-42 were reduced by 68.2% ± 2.7% and 49.4 ± 0.9%, respectively (two-way analysis of variance $P < 0.0001$ for the effect of Aβ1-40 versus Aβ1-42) (Supplemental Figure S4C).

Furthermore, we analyzed the rate of intracellular degradation of internalized Aβ by astrocytes akin to the experiment in which we compared the rate of intraneuronal degradation of Aβ between primary hippocampal neurons cultured alone and those co-cultured with astrocytes. After 6 hours of exposure to 10 μmol/L Aβ1-40, the Aβ1-40 signal was seen only in the astrocytic lysate at the conclusion of the Aβ exposure, whereas no Aβ1-40 signal was detectable within t = 2 hours after commencement of the washout period (Supplemental Figure S4D). These experiments confirmed robust Aβ clearance and intracellular degradation capacity of astrocytes.

Confocal Microscopy Analysis of Aβ1-40 Accumulation and Distribution in the Primary Hippocampal Neurons Cultured Alone and Those Co-Cultured with Astrocytes without and with Aβ12-28P Treatment

Along with biochemical analysis of the intracellular Aβ content, we have used confocal microscopy to directly image differences in the intracellular accumulation and distribution of Aβ between primary hippocampal neurons cultured alone and those co-cultured with astrocytes. In the

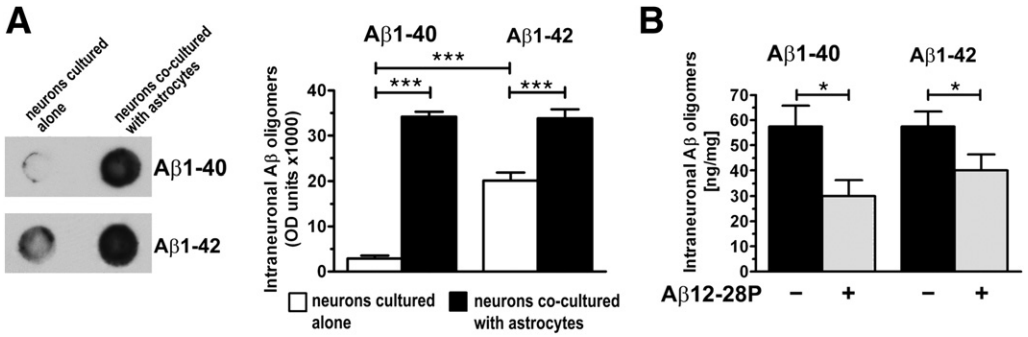

Figure 3 Analysis of intraneuronal content of Aβ oligomers. **A**: Representative dot immunoblots developed with the use of A11 oligomer-specific antibody from lysates of primary hippocampal neurons cultured alone and those co-cultured with astrocytes, after exposure to Aβ1-40 and Aβ1-42. Values in the graphs show the mean dot blot optic densities ± SEM in four independent experiments (one-way analysis of variance $P < 0.0001$). Values of post hoc pair analysis conducted with Tukey's HSD test are displayed on the graph if statistically significant. **B**: Levels of intraneuronal Aβ1-40 and Aβ1-42 oligomers in primary hippocampal neurons co-cultured with astrocytes without or with Aβ12-28P treatment quantified with ELISA specific for aggregated human Aβ and expressed in nanograms of Aβ per milligram of the total protein in cell lysate. Values are given as means ± SEM from five independent experiments. The *U*-test was used to analyze statistical significance of the Aβ12-28P treatment separately for Aβ1-40 and Aβ1-42. $*P < 0.05$, $***P < 0.001$.

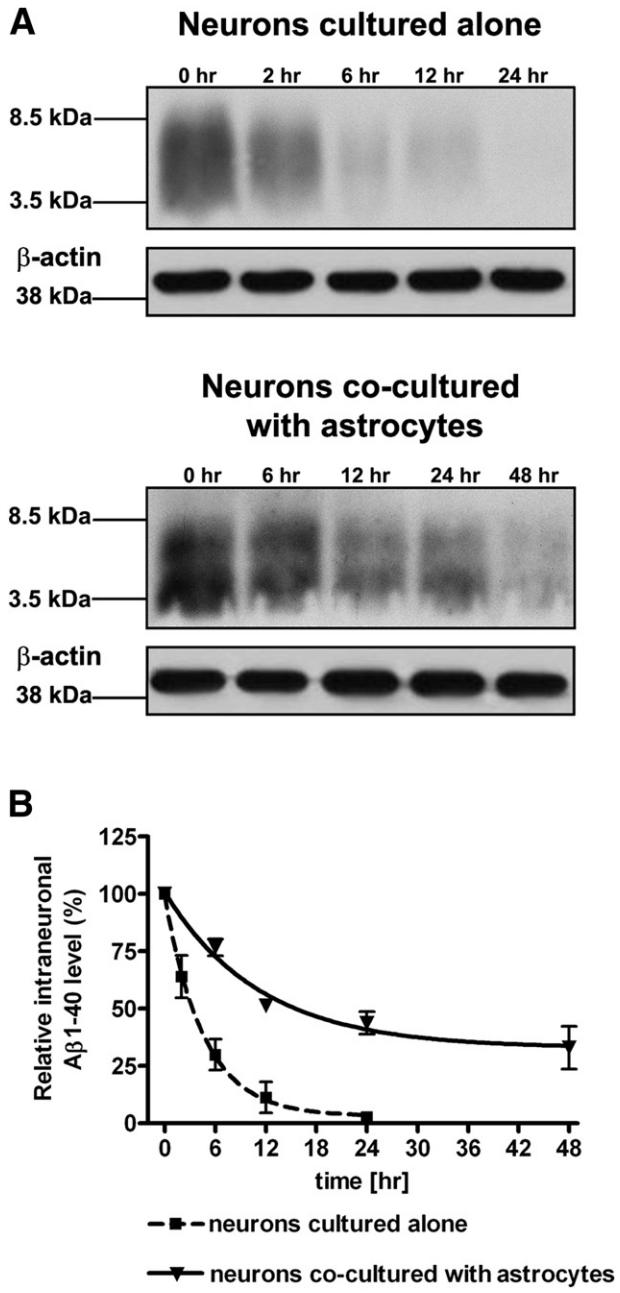

Figure 4 Intraneuronal degradation of internalized Aβ1-40. **A:** Representative Western immunoblot analysis for Aβ1-40 in lysates of primary hippocampal neurons cultured alone (**top panel**) and co-cultured with astrocytes (**bottom panel**) at various time points during the washout period after 6 hours of exposure to Aβ1-40; densitometric analysis is depicted in **B.** Also included are Western immunoblot analyses for β-actin, which was used as a loading control. **B:** Intraneuronal levels of Aβ1-40 during the washout period. Data expressed as the mean percentage ± SEM of Aβ band optic densities relative to those at t = 0 hours (conclusion of the exposure to Aβ1-40) from five independent experiments.

confocal microscopy experiments, Aβ1-40 added to the culture medium was traced with 10% FITC-Aβ1-40, which allowed us to directly visualized Aβ accumulation and distribution. The Aβ1-40/FITC-Aβ1-40 mixture was added to the conditioned media once at the commencement of the experiment at the final concentration of 10 μmol/L, and the neurons were cultured in its presence for 72 hours. In primary hippocampal neurons cultured alone, most of the Aβ1-40 was found outside neurons visible in the form of fine aggregates that covered the external surface of their dendrites (Figure 5A). A small amount of Aβ1-40 was also found inside neuronal perikarya (Figure 5, B and C). In contrast, in neurons co-cultured with astrocytes, a significantly smaller number of Aβ1-40 aggregates were seen on the external surface of dendrites (Figure 5D). Instead, confocal microscopy tomograms taken at the level of perikarya showed large Aβ1-40 aggregates present inside the neurons. They were clearly visualized inside the perikarya and in proximal segments of the primary dendrites (Figure 5, E and F). Intraneuronal Aβ aggregates stained negatively with thioflavin-S, which indicated that they contain no fibrillar Aβ (not shown). In the treatment experiment, 10 μmol/L Aβ12-28P was added together with Aβ1-40/FITC-Aβ1-40 to the neuronal-astrocytic co-cultures at the commencement of the experiment. Under Aβ12-28P treatment, the amount of intraneuronal Aβ1-40 aggregates was greatly reduced (Figure 5, G–I).

Furthermore, we combined confocal microscopy with immunocytochemistry against organelle-specific markers to analyze the subcellular distribution of internalized Aβ1-40 in primary hippocampal neurons when they were cultured alone or co-cultured with astrocytes without and with Aβ12-28P treatment. As in the previous experiments, neuronal monocultures and neuronal-astrocytic co-cultures were maintained in the presence of Aβ1-40 traced with 10% FITC-Aβ1-40 (10 μmol/L final Aβ1-40/FITC-Aβ1-40 concentration) for 72 hours. At the conclusion of the experiment, they were fixed and immunostained against early endosome antigen 1 early endosomal marker, Rab7 late endosomal marker, Cathepsin D late endosomal and lysosomal marker, and heat shock protein 60 as a mitochondrial marker. Primary hippocampal neurons cultured alone showed a modest amount of intraneuronal Aβ1-40, which colocalized weakly with all four organelle markers (Figure 6, A and B, and Supplemental Figure S5, A and B). In contrast neurons co-cultured with astrocytes showed a substantial increase in the intraneuronal content of Aβ1-40 compared with neurons cultured alone. In neurons from the neuronal-astrocytic co-cultures, the Aβ1-40 content was particularly increased in late endosomes and in lysosomes (Figure 6C and Supplemental Figure S5C). To less extent, Aβ1-40 colocalized with markers for early endosomes and mitochondria. Furthermore, some Aβ1-40 was seen outside the nuclear envelope and did not show colocalization with any of the aforementioned organelle markers, which suggested its possible cytoplasmic localization. As in previous experiments, Aβ12-28P treatment of primary hippocampal neurons co-cultured with astrocytes resulted in a marked reduction in the intraneuronal Aβ accumulation in all investigated organelles and cytoplasm (Figure 6D and Supplemental Figure S5D).

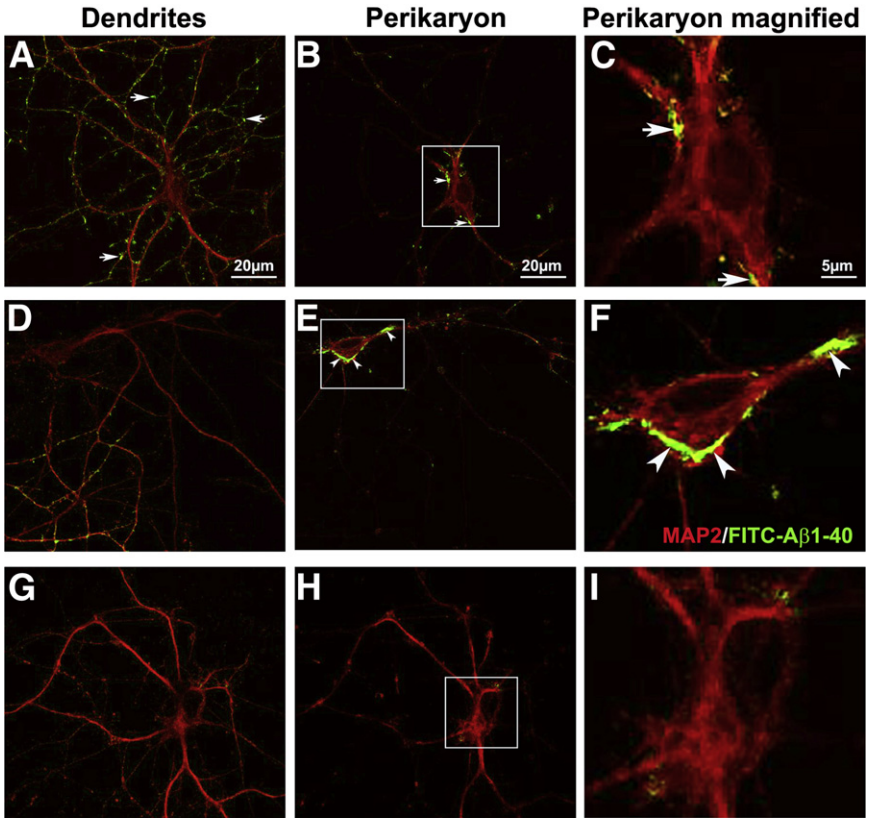

Figure 5 Confocal microscopy analysis of Aβ1-40 distribution and accumulation in the primary hippocampal neurons. **A**: A tomographic cross section through the level of the dendritic tree of a representative primary hippocampal neuron from a monoculture grown in the presence of Aβ1-40 in the conditioned media. Aβ1-40 was traced with 10% of FITC-Aβ1-40. **Arrows** show fine Aβ1-40 aggregates that decorate the outer surface of the dendrites. **B** and **C**: A tomographic cross section through the level of the perykaryon of the same neuron. **Arrows** indicate sparse intraneuronal Aβ1-40 aggregates in the perykaryon and in proximal segments of primary dendrites. **D**, **E**, and **F**: A representative primary hippocampal neuron from a neuronal-astrocytic co-culture grown in the presence of Aβ1-40/FITC-Aβ1-40. **Arrowheads** indicate large Aβ1-40 aggregates in the perykarion and in the proximal segments of dendrites. **G**, **H**, and **I**: A representative primary hippocampal neuron grown in co-culture with astrocytes and treated with Aβ12-28P during exposure to Aβ1-40/FITC-Aβ1-40, showing a marked reduction in the intraneuronal Aβ accumulation. Neurons were identified by anti–microtubule-associated protein (MAP) 2 immunostaining (red) whereas green color represents FITC-Aβ1-40 fluorescence. All shown confocal tomograms are 1 μm thick. Tomograms through the perikaryon were taken 5 to 6 μm above the level of tomograms showing dendritic tree. Scale bars: 20 μm (**A** and **B**); 5 μm (**C**).

Primary Hippocampal Neurons Co-Cultured with Astrocytes Show Enhanced Loss of Synaptic Proteins During Exposure to Aβ1-40, Which Can Be Inhibited by Aβ12-28P Treatment

To investigate whether increased intraneuronal accumulation and oligomerization of Aβ by primary hippocampal neurons co-cultured with astrocytes is associated with enhanced synaptic degeneration, we determined surface expression of the following synaptic proteins: NR1 subunit of the NMDAR, PSD-95, and synaptophysin. Quantification of synaptic protein expression was performed in 18-DIV primary hippocampal neurons cultured alone or co-cultured with astrocytes after 72 hours of exposure to Aβ1-40 traced with 10% FITC-Aβ1-40 (10μmol/L final concentration), without and with Aβ12-28P cotreatment. In primary hippocampal neurons cultured alone, exposure to Aβ1-40 resulted in significant down-regulation of the NR1 subunit of NMDAR, PSD-95, and synaptophysin expression by 46.3%, 51.9%, 54.4% of the control neuron expression, respectively ($P < 0.001$) (Figure 7, A, B, and F). In primary hippocampal neurons cultured alone, loss of synaptic proteins expression was mainly associated with the presence of Aβ1-40 aggregates that covered the external surfaces of the dendrites (Figure 7B), whereas the amount of intraneuronally accumulated Aβ was modest.

Co-culturing of primary hippocampal neurons with astrocytes in the absence of Aβ1-40 was associated with marked up-regulation of PSD-95 and synaptophysin expression compared with primary hippocampal neurons cultured alone by 21.7% and 12.2%, respectively ($P < 0.001$) (Figure 7, C and F), whereas no statistically significant difference in the expression of NMDAR NR1 subunit was observed (Figure 7, C and F). When primary hippocampal neurons grown in co-cultures with astrocytes were exposed to Aβ1-40, the reduction in the synaptic protein expression was markedly greater than that observed in primary hippocampal neurons cultured alone. Expression of NR1, PSD-95, and synaptophysin was reduced by 76.8%, 80.4%, and 75.3%, respectively, compared with neurons grown in co-cultures with astrocytes in the absence of Aβ1-40 ($P < 0.001$) (Figure 7, D and F). This profound loss of synaptic protein expression was associated with massive intraneuronal Aβ1-40 accumulation (Figure 7D). The loss of synaptic protein markers was not associated with degeneration of the cytoskeleton as shown with the use of α-tubulin, as a control cytoskeletal protein. The Western immunoblot signals for α-tubulin in lysates of primary hippocampal neurons treated with Aβ1-40 in the absence or presence of astrocytes were comparable with those of control neurons (Supplemental Figure S6). Aβ12-28P treatment of neurons co-cultured with astrocytes inhibited the loss of synaptic proteins. Compared with the primary hippocampal neurons co-cultured with astrocytes in the absence of Aβ1-40, expression of the NR1 subunit of NMDAR, PSD-95, and synaptophysin was reduced only by 29%, 26.1%, and 36.5%, respectively ($P < 0.001$) (Figure 7, E and F). The therapeutic effect of Aβ12-28P on synaptic protein

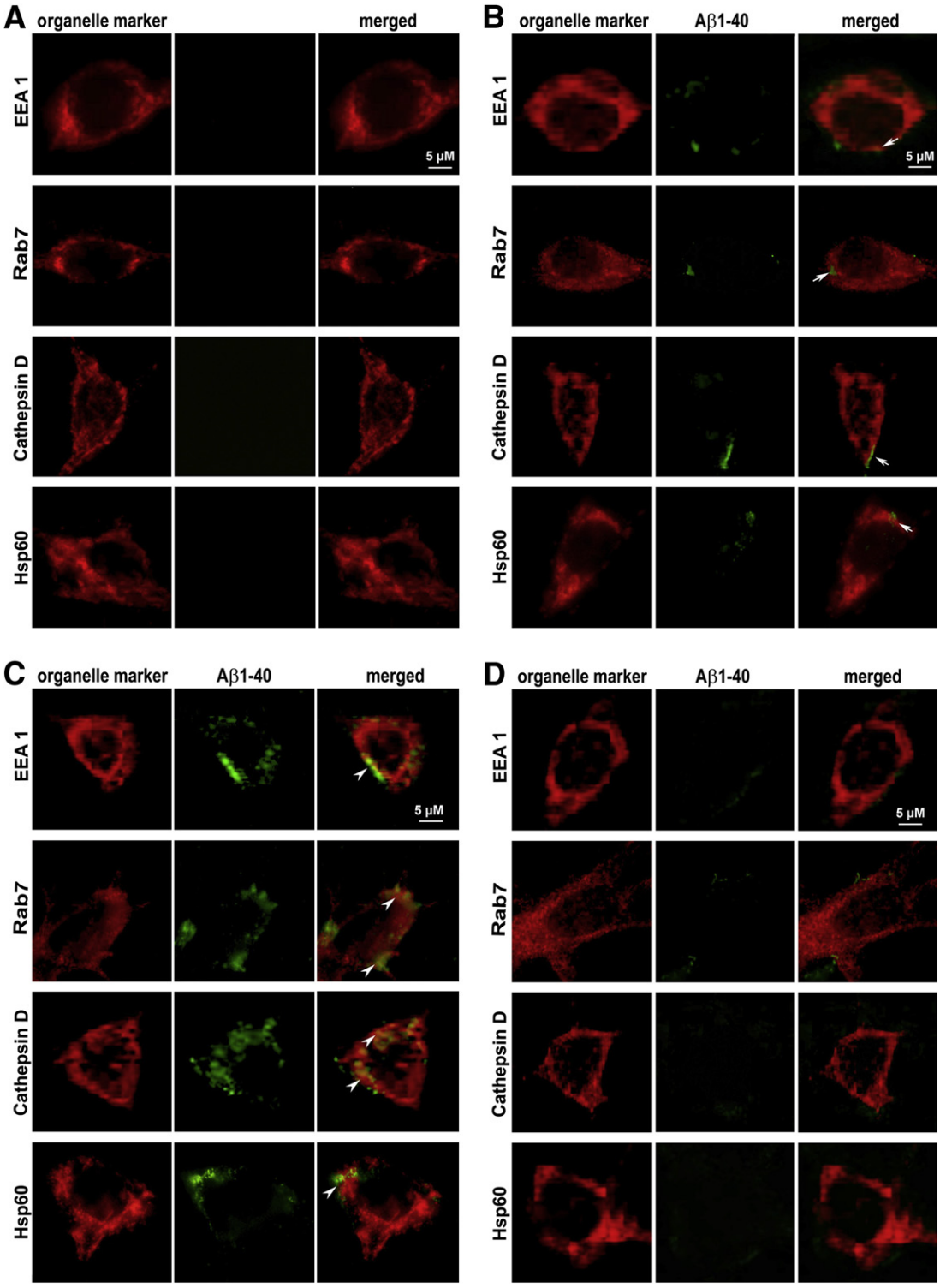

Figure 6 Subcellular distribution of internalized Aβ1-40 in primary hippocampal neurons. **A:** Representative microphotographs of control primary hippocampal neurons cultured alone and immunostained against specific intracellular organelle markers: early endosome antigen 1 (EEA1) for early endosomes, Rab7 for late endosomes, Cathepsin D for late endosomes and lysosomes, and heat shock protein 60 (HSP60) for mitochondria. **B:** Representative microphotographs of primary hippocampal neurons cultured alone in the presence of Aβ1-40 (traced with 10% of FITC-Aβ1-40). **Arrows** indicate weak colocalization of internalized Aβ1-40 with EEA1, Rab7, Cathepsin D, and HSP60. **C:** Representative microphotographs of primary hippocampal neurons co-cultured with astrocytes in the presence of Aβ1-40/FITC-Aβ1-40. **Arrowheads** indicate ample amount of intraneuronal Aβ1-40 showing colocalization with Rab7 and Cathepsin D and, to less extent, with HSP60 and EEA1. **D:** Representative microphotographs of primary hippocampal neurons co-cultured with astrocytes that were treated with Aβ12-28P during the exposure to Aβ1-40/FITC-Aβ1-40. There is markedly reduced intraneuronal Aβ1-40 content, especially in the late endosomes and lysosomes. Red color represents immunostaining against specific intracellular organelle markers, whereas green is FITC-Aβ1-40. Scale bars: 5 μM (**A**—**D**).

expression was associated with substantial reduction in the intraneuronal Aβ1-40 accumulation (Figure 7E).

Knockout of the *Apoe* Gene in $APP_{SW}/PS1_{dE9}$AD Tg Mice Results in the Absence of Extracellular Fibrillar Aβ Deposits, Whereas TR with ApoE4 Isoform Doubles the Load of Fibrillar Aβ Deposits Compared with TR with ApoE2 and ApoE3 Isoforms

To investigate the role of ApoE in the *in vivo* intraneuronal Aβ accumulation, we have generated four novel AD Tg mice lines, including $APP_{SW}/PS1_{dE9}$/ApoE2, $APP_{SW}/PS1_{dE9}$/ApoE3, $APP_{SW}/PS1_{dE9}$/ApoE4, and $APP_{SW}/PS1_{dE9}$/ApoE KO. These Tg mice were derived from ApoE-TR mice, where human ApoE isoforms are expressed at the physiological levels of murine ApoE expression.[18,19] For the first time, we have quantified deposition of extracellular Aβ in these previously uncharacterized AD Tg mice lines, calculating the average load of fibrillar Aβ deposits in the neocortex in 11-month-old female mice with the use of an unbiased stereologic principle. The mean fibrillar Aβ load in $APP_{SW}/PS1_{dE9}$/ApoE2 mice and $APP_{SW}PS1_{dE9}$/ApoE3 was 0.86% ± 0.19% and 1.05% ± 0.18%, respectively (Figure 8, A and B) (difference not statistically significant). In $APP_{SW}/PS1_{dE9}$/ApoE4, the fibrillar Aβ load was 1.92% ± 0.34%, almost twice as high as in mice expressing E2 and E3 isoforms ($P < 0.05$). $APP_{SW}PS1_{dE9}$/ApoE KO mice had little true amyloid deposits shown by amyloid-binding dyes X-34 or thioflavin-S. Scant deposits were too rare and too small to be reliably thresholded and quantified (Figure 8A). A fair number of nonfibrillar Aβ deposits could be shown in $APP_{SW}PS1_{dE9}$/ApoE KO mice with the use of anti-Aβ immunohistochemistry (Figure 8C). In the various lines of $APP_{SW}PS1_{dE9}$/ApoE-TR mice differences in the load of Aβ deposits shown by immunohistochemistry corresponded to that noted by amyloid-binding dyes.

Knockout of the *Apoe* Gene in $APP_{SW}/PS1_{dE9}$AD Tg Mice Markedly Reduces Intraneuronal Aβ Presence Compared with TR with Human ApoE Isoforms

The effect of ApoE KO and expression of various human ApoE isoforms on intraneuronal Aβ presence was investigated by confocal microscopy in the pyramidal neurons in the CA1 and CA2/CA3 sectors of the cornu ammonis with the use of double immunostaining against $Aβ_{1-X}$ and MAP2 for neuronal identification. $Aβ_{1-X}$ was immunostained with 6E10/4G8 mAbs that gave a bright punctate immunostaining pattern inside perikarya (Figure 9A). In $APP_{SW}/PS1_{dE9}$/ApoE KO mice few neurons showed intraneuronal $Aβ_{1-X}$ presence. They constituted 1.2% ± 0.3% and 4.3% ± 0.6%, respectively, of the total population of pyramidal neurons in the CA1 and CA2/3 sectors ($P < 0.001$ against all $APP_{SW}/PS1_{dE9}$/ApoE-TR lines) (Figure 9B). In $APP_{SW}/PS1_{dE9}$/ApoE-TR mice, the percentage of CA1 neurons with intraneuronal $Aβ_{1-X}$ presence ranged from 39.7% ± 2.3% in $APP_{SW}/PS1_{dE9}$/ApoE2 mice to 45.4% ± 1.6% in the $APP_{SW}/PS1_{dE9}$/ApoE4 line. In the CA2/3 sector, the percentage of $Aβ_{1-X}$-positive neurons ranged from 55.9% ± 2.0% in the $APP_{SW}/PS1_{dE9}$/ApoE3 line to 63.1% ± 2.3% in the $APP_{SW}/PS1_{dE9}$/ApoE4 line. The fraction of pyramidal neurons that showed intraneuronal $Aβ_{1-X}$ presence was significantly higher in the CA2/3 sector than in the CA1 sector for all ApoE isoforms ($P < 0.001$) but not in $APP_{SW}/PS1_{dE9}$/ApoE KO mice. Statistically significant differences between particular ApoE isoforms were seen only in the CA2/3 sector between $APP_{SW}PS1_{dE9}$/ApoE2 and $APP_{SW}PS1_{dE9}$/ApoE4 mice ($P < 0.01$). To show specific immunodetection of intraneuronal Aβ presence with a mixture of 6E10 and 4G8 mAbs, with no conflicting signals from APP, additional sections were immunostained with mAb HJ7.4 against the carboxy terminus of $Aβ_{X-42}$ and Abs against carboxy and amino termini of APP (Figure 9C). $Aβ_{X-42}$ carboxy-terminal immunostaining produced a fine, granular pattern that was associated with a large fraction of pyramidal neurons in $APP_{SW}/PS1_{dE9}$/ApoE-TR mice but with few neurons in $APP_{SW}/PS1_{dE9}$/ApoE KO mice, akin to that observed with 6E10/4G8 mAb staining. Both anti-APP Abs produced robust staining of virtually all CA1 and CA2/3 pyramidal neurons in $APP_{SW}/PS1_{dE9}$/ApoE KO mice, which was comparable with that seen in $APP_{SW}/PS1_{dE9}$/ApoE-TR mice.

Discussion

Intraneuronal accumulation of Aβ is a potentially important aspect of AD pathogenesis. Intraneuronal Aβ is derived from Aβ internalized by neurons from the extracellular space through ApoE-dependent and ApoE-independent uptakes and from intrinsic Aβ that escapes exocytosis after APP cleavage that takes place in the endocytic compartment.[34] Disequilibrium between the rate of intraneuronal Aβ accumulation and intraneuronal Aβ degradation in AD neurons results in its intraneuronal buildup. This equilibrium is further affected by Aβ clearance into cerebrospinal fluid and across the BBB.[35] Through its high affinity for Aβ and receptor-mediated clearance, ApoE contributes importantly to Aβ metabolism and intraneuronal uptake. To better characterize effects of astrocyte-derived ApoE on the intraneuronal Aβ accumulation and to test a hypothesis that an ApoE/Aβ antagonist would effectively lower intraneuronal Aβ level, we set up a noncontact, neuronal-astrocytic co-culture model. With the use of this model system, we found significantly increased intraneuronal accumulation of Aβ peptides in primary hippocampal neurons co-cultured with astrocytes compared with neurons cultured alone during exposure to synthetic Aβ peptides in the conditioned media. To ascertain that the observed effect depends specifically on ApoE, we compared intraneuronal Aβ1-42 levels between primary hippocampal neurons co-cultured with ApoE KO astrocytes and primary hippocampal neurons cultured alone and found no significant differences. We found that the intraneuronal level of Aβ1-40 and Aβ1-42 in primary

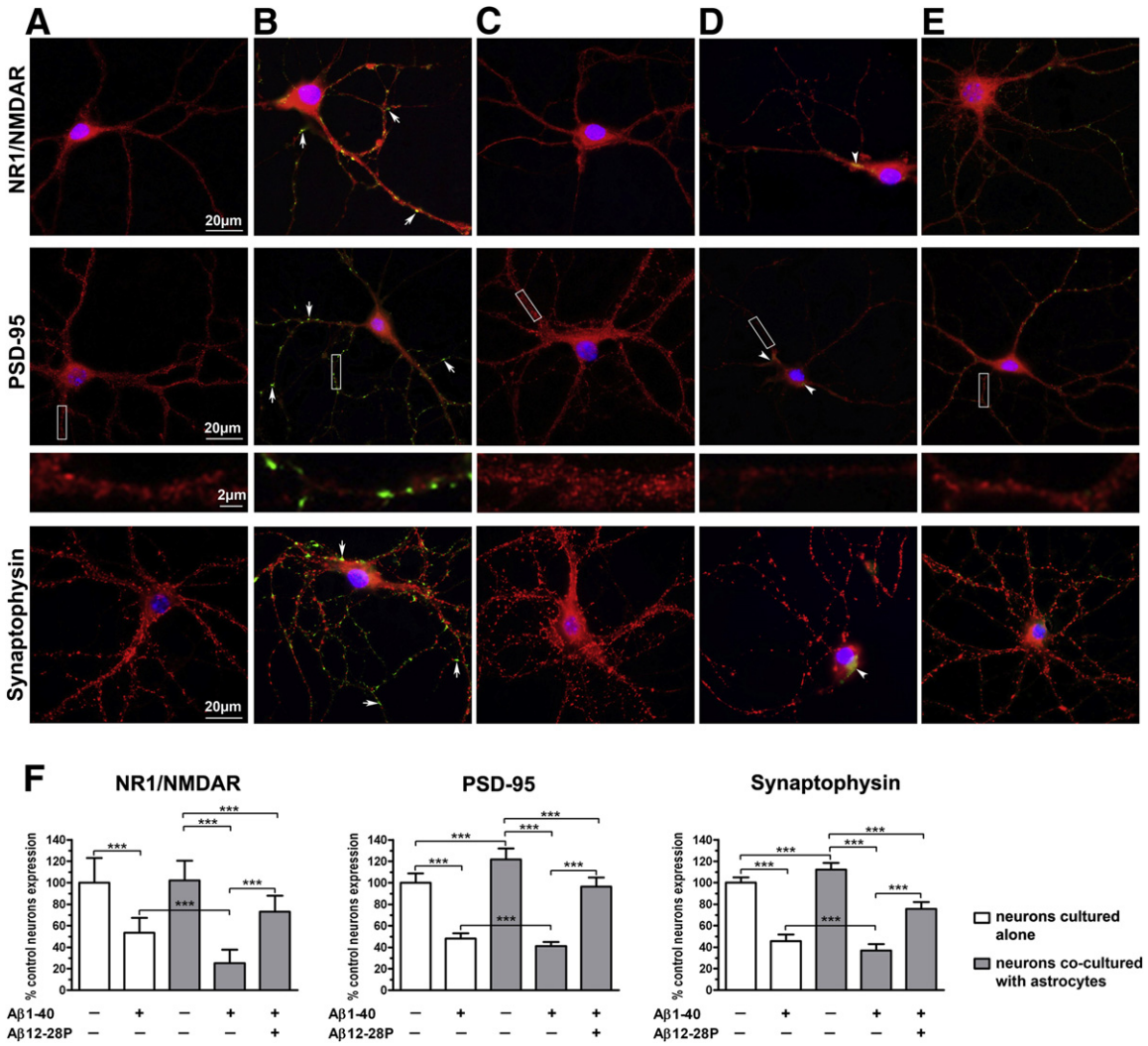

Figure 7 Expression of synaptic protein markers in primary hippocampal neurons. **A** and **B**: Representative microphotographs of primary hippocampal neurons immunostained against NR1 subunit of the *N*-methyl-D-aspartic acid receptor (NMDAR), postsynaptic density protein 95 (PSD-95), and synaptophysin, which were cultured alone in the absence and presence of Aβ1-40 traced with 10% of FITC-Aβ1-40, respectively. **Arrows** in **B** indicate fine Aβ1-40 aggregates covering the external surface of the dendrites. **C** and **D**: Representative microphotographs of primary hippocampal neurons co-cultured with astrocytes in the absence and presence of Aβ1-40/FITC-Aβ1-40 in the conditioned media, respectively. **Arrowheads** in **D** indicate intraneuronal Aβ1-40 accumulation in the perykaryon and proximal segments of primary dendrites. **E**: Representative microphotographs of primary hippocampal neurons co-cultured with astrocytes in the presence of Aβ1-40/FITC-Aβ1-40 in the conditioned media, which were also cotreated with Aβ12-28P. Red color represents immunostaining against specific synaptic proteins, green is FITC-Aβ1-40, whereas blue is DAPI nuclear counterstaining. **Rectangular areas** covering section of dendrites of neurons immunostained against PSD-95 are enlarged directly underneath each image and represent example test fields selected for quantification of synaptic protein expression. For antibodies that control staining, see Supplemental Figure S3. **F**: Quantitative analysis of synaptic protein expression. Values show means ± SD density of synaptic proteins along primary and secondary dendrites relative to those in primary hippocampal neurons cultured alone without Aβ−40 in three independent experiments. One-way analysis of variance $P < 0.0001$ for all three synaptic proteins. Post hoc Tukey' s HSD test values are displayed on the graph for pairs of columns with statistically significant differences. ***$P < 0.001$. Scale bars: 20 μM (**A**); 2 μM (enlarged area in **A**).

hippocampal neurons co-cultured with astrocytes can be effectively lowered with Aβ12-28P, which is a well-established inhibitor of ApoE/Aβ binding,[16,22] but not with a peptide representing its scrambled sequence. Furthermore, Aβ12-28P treatment had no effect on the intraneuronal Aβ level in primary hippocampal neurons cultured alone, which again indicates that ApoE is required for its pharmacodynamic effect. The level of ApoE in the conditioned media was also verified and showed no significant variability among different treatment conditions, which could account for differences in the uptake of Aβ peptides from the media and their intraneuronal accumulation. As shown by us and others, ApoE facilitates but it is not required for Aβ uptake, because neurons grown in the absence of ApoE can internalize Aβ.[28] However, ApoE can greatly increase the tempo of Aβ internalization by binding Aβ in the extracellular space and directing it to neurons, which internalize ApoE/Aβ complexes through highly efficient receptor-mediated endocytosis. Besides finding a strong effect of ApoE on increasing the intraneuronal level of both Aβ1-40 and Aβ1-42, we also

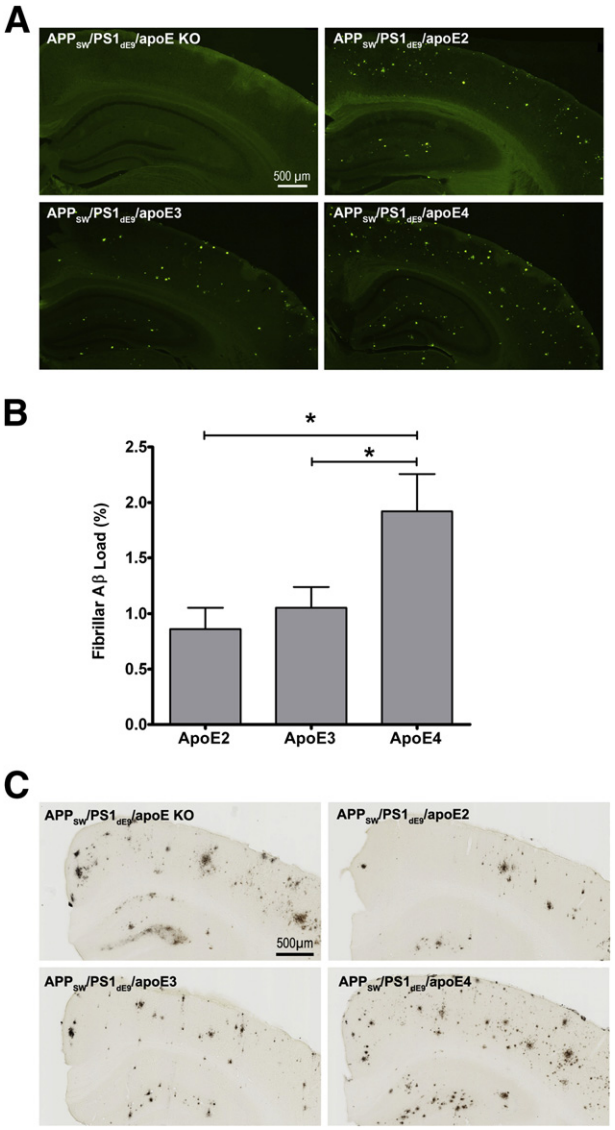

Figure 8 Analysis of extracellular Aβ deposits in APP_{SW}/PS_{dE9}/ApoE KO and APP_{SW}/PS_{dE9}/ApoE-TR lines. **A**: Representative microphotographs of thioflavin-S–stained coronal brain sections from APP_{SW}/PS_{dE9}/ApoE KO and APP_{SW}/PS_{dE9}/ApoE-TR mice involving the hippocampus, the cingulate cortex, and the somatosensory cortex. **B**: Unbiased quantification of the fibrillar Aβ load in the neocortex of 11-month-old female APP_{SW}/PS_{dE9}/ApoE-TR mice, which are homozygotes for E2, E3, and E4 alleles. Values are given as means ± SEM ($n = 8$ per group). Statistical significance between particular transgenic lines was analyzed with *U*-test, whose values, if significant, are depicted in the figure. $^*P < 0.05$. **C**: Representative microphotographs of coronal brain sections involving the hippocampus, the cingulated cortex, and the somatosensory cortex, which were immunostained against $Aβ_{1-X}$. Scale bars: 500 μM (**A** and **C**).

showed that ApoE promotes intraneuronal oligomerization of both Aβ1-40 and Aβ1-42 peptides and impairs intraneuronal Aβ1-40 clearance. Unlike the well-recognized effect of ApoE on promoting Aβ fibrillization,[36] its effect on Aβ oligomerization has been underappreciated until recently. Several recent studies provided evidence to support increased content of Aβ oligomers in the extracellular space in brains of patients with AD, expressing the human ApoE4 isoform,[37,38] and intraneuronally in mice expressing human ApoE4 isoform after inhibition of Aβ-degrading enzyme neprilysin.[39]

Because various ApoE receptors play an important role in Aβ metabolism, the effect of their overexpression on Aβ pathology has been studied with various model systems. Overexpression of low-density lipoprotein receptor-related protein (LRP) in several neuronal cell lines resulted in increased intraneuronal Aβ accumulation.[15,40] LRP overexpression in APP_{V717F} mice, besides augmenting intraneuronal Aβ accumulation, exacerbated the memory deficit and caused an increase in soluble Aβ level in the brain.[41] A contrasting effect was seen in $APP_{SW}/PS1_{dE9}$/LDLR mice that overexpress low-density lipoprotein receptor (LDLR), which together with LRP constitute two main ApoE receptors in the brain. $APP_{SW}/PS1_{dE9}$/LDLR mice showed increased clearance of Aβ from the extracellular space and inhibition of Aβ deposition.[21] These mice overexpress LDLR in neurons and astrocytes, which indicates that the protective effect of LDLR up-regulation can be related to the receptor subtype and/or its overexpression in nonneuronal cells capable of efficient Aβ degradation.[42] In addition, treatment of several AD Tg mice models with liver X receptor or retinoid X receptor agonists, which up-regulate ApoE expression and enhance its lipidation status, resulted in reduction of Aβ plaque load through enhancing clearance of Aβ by glial cells.[43,44] These published data indicate that the ApoE/Aβ interaction may result in multidirectional effects that may promote Aβ degradation by nonneuronal cells[43,44] while enhancing Aβ accumulation in neurons. In our studies, we analyzed levels of Aβ peptides in the conditioned media at the conclusion of the experiment, and we found that their levels in the co-culture systems are markedly lower than those in neuronal monocultures. This difference may be explained by the presence of astrocytes in the co-culture system, which shows robust capacity for clearance of Aβ from extracellular space and its intracellular degradation. Thus, neurons co-cultured with astrocytes appear to accumulate more Aβ internally despite reduction in Aβ level in the condition media, which implies that astrocytes play a double-edged sword role by clearing Aβ from the media and at the same time producing ApoE that promotes intraneuronal Aβ accumulation. Aβ12-28P treatment of neurons co-cultured with astrocytes reduced the intraneuronal levels of Aβ peptides below that detected in neurons cultured alone, because it blocked ApoE-mediated Aβ internalization, whereas ApoE-independent Aβ uptake was limited because of reduced Aβ concentration in the conditioned media.

Confocal microscopy imaging of neurons from astrocytic co-cultures showed increased Aβ content in the endosomal/lysosomal compartment, which is consistent with internalization of ApoE/Aβ complexes through receptor-mediated endocytosis, directing the complex to the endosomal/lysosomal system. Consistent with our current observations, overexpression of LRP facilitated endocytosis of

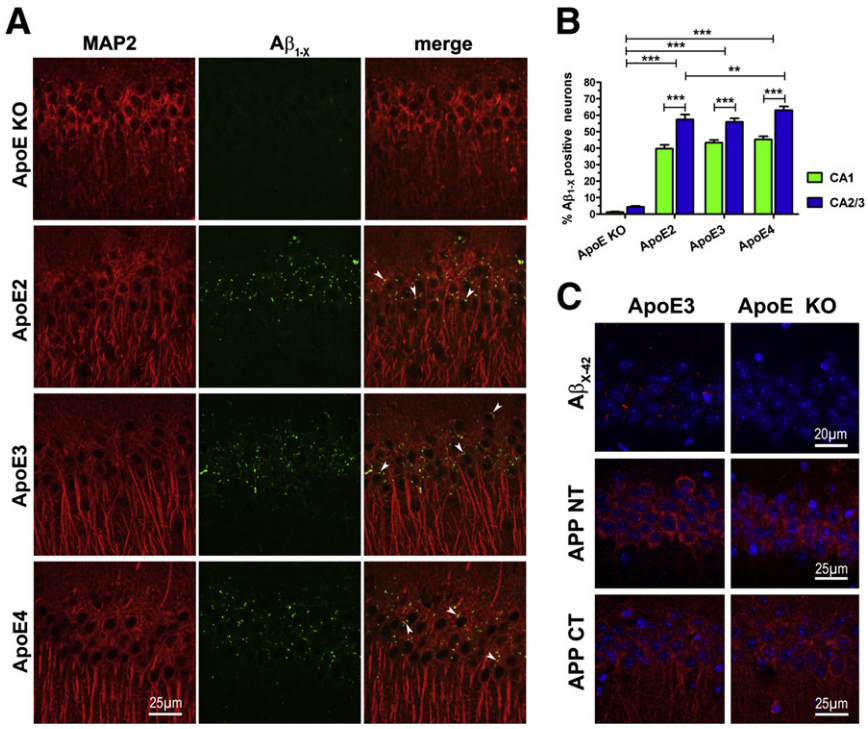

Figure 9 Analysis of intraneuronal Aβ accumulation in APP_{SW}/PS_{dE9}/ApoE KO and APP_{SW}/PS_{dE9}/ApoE-TR lines. **A:** Representative confocal microscopy images 1 μm thick through the body of pyramidal neurons in the CA1 sector of the cornu ammonis immunostained with a mixture of 6E10/4G8 monoclonal antibodies against intraneuronal $Aβ_{1-X}$ (green channel). Neurons were identified by MAP2 immunostaining (red channel). **Arrowheads** indicate intraneuronal aggregates of $Aβ_{1-X}$. **B:** Quantitative analysis of $Aβ_{1-X}$-positive neurons in the CA1 and CA2/CA3 sectors of the cornu ammonis in APP_{SW}/PS_{dE9}/ApoE KO and APP_{SW}/PS_{dE9}/ApoE-TR lines. Analysis of variance $P < 0.0001$ for both sectors and ApoE isoform effect. Values of the post hoc analysis that used Bonferroni's test are displayed on the graph for pairs of columns with statistically significant differences. $^{**}P < 0.01$, $^{***}P < 0.001$. **C:** Comparison of immunostainings with monoclonal antibody HJ7.4 against carboxy terminus of $Aβ_{X-42}$ and antibodies against amino or carboxy termini of APP (red) with DAPI counterstaining (blue) in CA1 pyramidal layer neurons in APP_{SW}/PS_{dE9}/ApoE3 and APP_{SW}/PS_{dE9}/ApoE KO lines. For antibody control staining, see Supplemental Figure S3. APP, amyloid precursor protein; CT, carboxy terminus; NT, amino terminus; MAP2, microtubule-associated protein 2. Scale bars: 25 μm (**A** and **C** $Aβ_{X-42}$); 25 μm (**C** APP NT and APP CT).

ApoE-containing lipid particles in APP_{V717F} mice, resulting in marked increase in the intraneuronal Aβ content, which colocalized with the lysosomal-associated membrane protein 1 lysosomal marker.[15] In contrast, evidence suggests that internalization of Aβ not associated with ApoE occurs through nonendocytotic mechanisms, which are based on the translocation of the cell surface bound Aβ directly to the cytosol and results in accumulation of Aβ primarily outside the endosomal/lysosomal compartment.[28,45,46]

Synapses, and in particular excitatory synapses of hippocampal neurons, are early targets of Aβ toxicity. Synaptotoxicity appears to concern both extracellular and intracellular Aβ. We showed that the loss of the NMDAR NR1 subunit, PSD-95, and synaptophysin expression in neuronal monocultures where confocal microscopy detected mainly extraneuronal Aβ1-40 aggregates, whereas more pronounced loss of these synaptic proteins was seen in neurons co-cultured with astrocytes, which also showed marked buildup of intraneuronal oligomers. It has been previously reported that extracellular application of Aβ oligomers to primary neuronal cultures or organotypic hippocampal slices induce rapid changes in the structure and density of synaptic spines[47,48] and reduces expression of NMDARs and related synaptic proteins,[49] through several signaling pathways, one of which involves the α-7 nicotinic receptor.[49] Loss of the NMDAR NR1 subunit and PSD-95 was also found in cultures of primary hippocampal neurons derived from APP_{SW} mice. These cultures are characterized by progressive buildup of intraneuronal Aβ, which is derived from endogenous Aβ escaping exocytosis after cleavage of the APP_{SW} mutant.[9,49] In this model, Aβ accumulates along the endosomal/lysomal pathway that leads to dysfunction of multivesicular bodies, causing impairment of the ubiquitin-proteasome system,[9] which also controls the fate of NMDARs undergoing endocytic vesicular trafficking.[50] ApoE-promoted buildup of Aβ oligomers along the endosomal/lysosomal pathway may therefore affect intracellular trafficking and sorting of synaptic proteins and may indicate a way in which intracellular Aβ contributes to synaptic degeneration. Furthermore, several AD Tg animal models are characterized by early and massive intraneuronal accumulation of Aβ oligomers, loss of synaptic proteins, and behavioral impairment which occur in the absence of extracellular Aβ plaques.[7,51] In particular, in 3×Tg-AD mice ($APP_{SW}/PS1_{M146V}/Tau_{P301L}$), intraneuronal Aβ accumulation may predate formation of Aβ plaques and neurofibrillary pathology and shows temporal correlation with synaptic dysfunction, emphasizing the role of intraneuronal Aβ in neurodegeneration.[52,53]

The *APOE* alleles are a well-recognized genetic risk factor for sporadic AD and correlate with severity of β-amyloidosis.[13] Inheritance of *APOE4* increases AD risk, whereas *APOE2* shows a relative protective effect. $APP_{SW}/PS1_{dE9}$/ApoE KO and $APP_{SW}/PS1_{dE9}$/ApoE-TR mice are new Tg lines produced to investigate the role of ApoE in Aβ pathology. The $APP_{SW}/PS1_{dE9}$ line represents a Tg model with enhanced disease phenotype, whereby the first plaques are detected by thioflavin-S at the age of 4 months.[54] Despite such aggressive development of Aβ pathology, the ApoE KO resulted in virtual absence of fibrillar Aβ deposits, which emphasizes a critical effect of ApoE on Aβ fibrillization and deposition. Similar effects of the ApoE KO were previously reported in APP_{V717F} and APP_{SW} lines, representing more latent models of Aβ pathology in which thioflavin-S detects

the first plaques around the age of 1 year.[14,55] TR of *APOE4* in $APP_{SW}/PS1_{dE9}$ mice was associated with a twofold increase in the load of extracellular Aβ deposits compared with TR of *APOE2* or *APOE3*, with all lines of mice showing substantial Aβ load at 11 months of age. Thus far, the differential effect of targeted ApoE isoform replacement on Aβ pathology has been reproduced in single APP_{V717F} mice, which had to be at least 18 months of age to observe substantial Aβ load.[56,57] Thus, $APP_{SW}/PS1_{dE9}$/ApoE-TR mice represent an important advance in modeling the effect of human ApoE isoforms on Aβ pathology, allowing us to conduct studies, for example, on novel AD therapeutics, in animals of much younger age.

ApoE KO in $APP_{SW}/PS1_{dE9}$ mice was associated with a marked reduction in intraneuronal Aβ presence. Because lack of ApoE should not have any effect on the non−ApoE-mediated pathways of Aβ uptake and accrual of endogenous Aβ remnants from APP cleavage, this experiment provides evidence to support the pivotal role of ApoE in intraneuronal Aβ accumulation, complementing our *ex vivo* data. For immunocytochemical detection of intraneuronal Aβ presence, we used a mixture of mAbs 6E10/4G8, which, although under certain conditions can cross-detect APP, in our staining gave primarily intraneuronal punctate pattern. This punctate pattern was different from the diffuse pattern of membrane staining seen when anti-APP antibodies were used in the control experiment. Furthermore, we have confirmed reduction in the intraneuronal Aβ presence associated with ApoE KO with the use of $Aβ_{X-42}$ C-terminal-specific mAb HJ7.4. Similar to observations in $APP_{SW}/PS1_{dE9}$/ApoE KO mice, KO of ApoE in APP_{V717F} mice was also reported to cause marked reduction in the intraneuronal Aβ accumulation.[15] Despite differences in the extraneuronal Aβ load, no significant effect of human ApoE isoforms on the number of Aβ-bearing neurons in $APP_{SW}/PS1_{dE9}$/ApoE-TR mice was observed, although it cannot be excluded that the actual intraneuronal Aβ level can vary between ApoE isoforms. As shown in another model involving inhibition of the Aβ-degrading enzyme neprilysin, intraneuronal oligomerization and accumulation of Aβ occurred more readily in mice that expressed the ApoE4 isoform than the ApoE3 isoform.[39]

We demonstrated that blocking the ApoE/Aβ interaction with the use of Aβ12-28P reduces intraneuronal Aβ1-40 and Aβ1-42 accumulation, including levels of intraneuronal Aβ1-40 and Aβ1-42 oligomers, and inhibits loss of synaptic proteins. Few other therapies have shown effects against intraneuronal Aβ. Limited examples include application of anti-Aβ mAbs into neuronal culture derived from APP_{SW} mice, whereby mAbs after binding to extracellular APP domain became internalized, resulting in reduced intraneuronal Aβ accumulation.[58] Although these *in vitro* observations indicate that anti-Aβ mAbs can be helpful in targeting intraneuronal Aβ, for *in vivo* application, limited BBB permeability of anti-Aβ mAbs may thwart their therapeutic potency in respect to lowering intraneuronal Aβ level, despite being effective in reducing Aβ plaque load, which primarily occurs through the peripheral sink mechanism.[59] In fact, transient clearance of intraneuronal Aβ in 3×Tg-AD mice was reported by intraventricularly but not systemically delivered immunotherapy.[53] Aβ12-28P is a nontoxic synthetic peptide that was modified for *in vivo* application, and its BBB permeability was previously evaluated and reported.[16] We have used Aβ12-28P in the past to successfully reduce Aβ plaques load and CAA in APP_{SW} and $APP_{SW}/PS1_{M146L}$ AD model mice.[22] Our previous and current experiments indicate that the antagonist of the ApoE/Aβ interaction can be effective in both reducing extracellular and intracellular Aβ deposition.

Acknowledgments

We thank Drs. Margaret and James I. Elliott (WM Keck Proteomic Facility of Yale University, New Haven, CT) for their outstanding proteomic services and Dr. Richard R. Kascsak (New York State Institute for Basic Research in Developmental Disabilities, Staten Island, NY) for providing 6E10 and 4G8 anti-Aβ monoclonal antibodies.

Supplemental Data

Supplemental material for this article can be found at *http://dx.doi.org/10.1016/j.ajpath.2013.01.034*.

References

1. Querfurth HW, LaFerla FM: Alzheimer's disease. N Engl J Med 2010, 362:329−344
2. Villemagne VL, Pike KE, Chetelat G, Ellis KA, Mulligan RS, Bourgeat P, Ackermann U, Jones G, Szoeke C, Salvado O, Martins R, O'Keefe G, Mathis CA, Klunk WE, Ames D, Masters CL, Rowe CC: Longitudinal assessment of Abeta and cognition in aging and Alzheimer disease. Ann Neurol 2011, 69:181−192
3. Tanzi RE, Moir RD, Wagner SL: Clearance of Alzheimer's A beta peptide: the many roads to perdition. Neuron 2004, 43:605−608
4. Stine WB, Dahlgren KN, Krafft GA, LaDu MJ: In vitro characterization of conditions for amyloid-beta peptide oligomerization and fibrillogenesis. J Biol Chem 2003, 278:11612−11622
5. Gouras GK, Tampellini D, Takahashi RH, Capetillo-Zarate E: Intraneuronal beta-amyloid accumulation and synapse pathology in Alzheimer's disease. Acta Neuropathol 2010, 119:523−541
6. LaFerla FM, Green KN, Oddo S: Intracellular amyloid-beta in Alzheimer's disease. Nat Rev Neurosci 2007, 8:499−509
7. Oakley H, Cole SL, Logan S, Maus E, Shao P, Craft J, Guillozet-Bongaarts A, Ohno M, Disterhoft J, Van EL, Berry R, Vassar R: Intraneuronal beta-amyloid aggregates, neurodegeneration, and neuron loss in transgenic mice with five familial Alzheimer's disease mutations: potential factors in amyloid plaque formation. J Neurosci 2006, 26:10129−10140
8. Takahashi RH, Capetillo-Zarate E, Lin MT, Milner TA, Gouras GK: Co-occurrence of Alzheimer's disease beta-amyloid and tau pathologies at synapses. Neurobiol Aging 2010, 31:1145−1152
9. Almeida CG, Takahashi RH, Gouras GK: Beta-amyloid accumulation impairs multivesicular body sorting by inhibiting the ubiquitin-proteasome system. J Neurosci 2006, 26:4277−4288
10. Almeida CG, Tampellini D, Takahashi RH, Greengard P, Lin MT, Snyder EM, Gouras GK: Beta-amyloid accumulation in APP mutant

neurons reduces PSD-95 and GluR1 in synapses. Neurobiol Dis 2005, 20:187–198
11. Lustbader JW, Cirilli M, Lin C, Xu HW, Takuma K, Wang N, Caspersen C, Chen X, Pollak S, Chaney M, Trinchese F, Liu S, Gunn-Moore F, Lue LF, Walker DG, Kuppusamy P, Zewier ZL, Arancio O, Stern D, Yan SS, Wu H: ABAD directly links Abeta to mitochondrial toxicity in Alzheimer's disease. Science 2004, 304:448–452
12. Zepa L, Frenkel M, Belinson H, Kariv-Inbal Z, Kayed R, Masliah E, Michaelson DM: ApoE4-driven accumulation of intraneuronal oligomerized Abeta42 following activation of the amyloid cascade in vivo is mediated by a gain of function. Int J Alzheimers Dis 2011, 2011: 792070
13. Kim J, Basak JM, Holtzman DM: The role of apolipoprotein E in Alzheimer's disease. Neuron 2009, 63:287–303
14. Bales KR, Verina T, Dodel RC, Du YS, Altstiel L, Bender M, Hyslop P, Johnstone EM, Little SP, Cummins DJ, Piccardo P, Ghetti B, Paul SM: Lack of apolipoprotein E dramatically reduces amyloid β-peptide deposition. Nat Genet 1997, 17:263–264
15. Zerbinatti CV, Wahrle SE, Kim H, Cam JA, Bales K, Paul SM, Holtzman DM, Bu GJ: Apolipoprotein E and low density lipoprotein receptor-related protein facilitate intraneuronal A beta 42 accumulation in amyloid model mice. J Biol Chem 2006, 281:36180–36186
16. Sadowski M, Pankiewicz J, Scholtzova H, Ripellino JA, Li YS, Schmidt SD, Mathews PM, Fryer JD, Holtzman DM, Sigurdsson EM, Wisniewski T: A synthetic peptide blocking the apolipoprotein E/beta-amyloid binding mitigates beta-amyloid toxicity and fibril formation in vitro and reduces beta-amyloid plaques in transgenic mice. Am J Pathol 2004, 165:937–948
17. Zhang H, Reddick RL, Piedrahita JA, Maeda N: Spontaneous hypercholesterolemia and arterial lesions in mice lacking apolipoprotein E. Science 1992, 258:468–471
18. Sullivan PM, Mezdour H, Aratani Y, Knouff C, Najib J, Reddick RL, Quarfordt SH, Maeda N: Targeted replacement of the mouse apolipoprotein E gene with the common human APOE3 allele enhances diet-induced hypercholesterolemia and atherosclerosis. J Biol Chem 1997, 272:17972–17980
19. Sullivan PM, Mezdour H, Quarfordt SH, Maeda N: Type III hyperlipoproteinemia and spontaneous atherosclerosis in mice resulting from gene replacement of mouse Apoe with human Apoe*2. J Clin Invest 1998, 102:130–135
20. Kim SW, Heo JH, Kim CH, Yoo DC, Won DH, Lee SG, Cho KJ, Song JH, Park SJ, Yang YG, Choi DW: Rapid and direct detection of apolipoprotein E genotypes using whole blood from humans. J Toxicol Environ Health A 2010, 73:1502–1510
21. Kim J, Castellano JM, Jiang H, Basak JM, Parsadanian M, Pham V, Mason SM, Paul SM, Holtzman DM: Overexpression of low-density lipoprotein receptor in the brain markedly inhibits amyloid deposition and increases extracellular A beta clearance. Neuron 2009, 64:632–644
22. Sadowski MJ, Pankiewicz J, Scholtzova H, Mehta PD, Prelli F, Quartermain D, Wisniewski T: Blocking the apolipoprotein E/amyloid-beta interaction as a potential therapeutic approach for Alzheimer's disease. Proc Natl Acad Sci U S A 2006, 103:18787–18792
23. Chromy BA, Nowak RJ, Lambert MP, Viola KL, Chang L, Velasco PT, Jones BW, Fernandez SJ, Lacor PN, Horowitz P, Finch CE, Krafft GA, Klein WL: Self-assembly of Abeta(1-42) into globular neurotoxins. Biochem 2003, 42:12749–12760
24. Lacor PN, Buniel MC, Chang L, Fernandez SJ, Gong Y, Viola KL, Lambert MP, Velasco PT, Bigio EH, Finch CE, Krafft GA, Klein WL: Synaptic targeting by Alzheimer's-related amyloid beta oligomers. J Neurosci 2004, 24:10191–10200
25. Mattson MP, Wang H, Michaelis EK: Developmental expression. compartmentalization, and possible role in excitotoxicity of a putative NMDA receptor protein in cultured hippocampal-neurons. Brain Res 1991, 565:94–108
26. Leroux PD, Reh TA: Reactive astroglia support primary dendritic but not axonal outgrowth from mouse cortical neurons in vitro. Exp Neurol 1996, 137:49–65
27. Carlson NG, Rojas MA, Black JD, Redd JW, Hille J, Hill KE, Rose JW: Microglial inhibition of neuroprotection by antagonists of the EP1 prostaglandin E2 receptor. J Neuroinflammation 2009, 6:5
28. Takuma K, Fang F, Zhang W, Yan S, Fukuzaki E, Du H, Sosunov A, McKhann G, Funatsu Y, Nakamichi N, Nagai T, Mizoguchi H, Ibi D, Hori O, Ogawa S, Stern DM, Yamada K, Yan SS: RAGE-mediated signaling contributes to intraneuronal transport of amyloid-beta and neuronal dysfunction. Proc Natl Acad Sci U S A 2009, 106:20021–20026
29. Wisniewski HM, Sadowski M, Jakubowska-Sadowska K, Tarnawski M, Wegiel J: Diffuse, lake-like amyloid-beta deposits in the parvopyramidal layer of the presubiculum in Alzheimer disease. J Neuropath Exp Neurol 1998, 57:674–683
30. Kim J, Jiang H, Park S, Eltorai AE, Stewart FR, Yoon H, Basak JM, Finn MB, Holtzman DM: Haploinsufficiency of human APOE reduces amyloid deposition in a mouse model of amyloid-beta amyloidosis. J Neurosci 2011, 31:18007–18012
31. Kayed R, Head E, Thompson JL, McIntire TM, Milton SC, Cotman CW, Glabe CG: Common structure of soluble amyloid oligomers implies common mechanism of pathogenesis. Science 2003, 300:486–489
32. Pankiewicz J, Prelli F, Sy MS, Kascsak RJ, Kascsak RB, Spinner DS, Carp RI, Meeker HC, Sadowski M, Wisniewski T: Clearance and prevention of prion infection in cell culture by anti-PrP antibodies. Eur J Neurosci 2006, 23:2635–2647
33. Sadowski MJ, Pankiewicz J, Prelli F, Scholtzova H, Spinner DS, Kascsak RB, Kascsak RJ, Wisniewski T: Anti-PrP Mab 6D11 suppresses PrP^{Sc} replication in prion infected myeloid precursor line FDC-P1/22L and in the lymphoreticular system in vivo. Neurobiol Dis 2009, 34:267–278
34. Takahashi RH, Almeida CG, Kearney PF, Yu FM, Lin MT, Milner TA, Gouras GK: Oligomerization of Alzheimer's beta-amyloid within processes and synapses of cultured neurons and brain. J Neurosci 2004, 24:3592–3599
35. Deane R, Wu ZH, Zlokovic BV: RAGE (Yin) versus LRP (Yang) balance regulates Alzheimer amyloid beta-peptide clearance through transport across the blood-brain barrier. Stroke 2004, 35:2628–2631
36. Ma J, Yee A, Brewer HB Jr, Das S, Potter H: Amyloid-associated proteins alpha 1-antichymotrypsin and apolipoprotein E promote assembly of Alzheimer beta-protein into filaments. Nature 1994, 372:92–94
37. Hashimoto T, Serrano-Pozo A, Hori Y, Adams KW, Takeda S, Banerji AO, Mitani A, Joyner D, Thyssen DH, Bacskai BJ, Frosch MP, Spires-Jones TL, Finn MB, Holtzman DM, Hyman BT: Apolipoprotein E, especially apolipoprotein E4, increases the oligomerization of amyloid beta peptide. J Neurosci 2012, 32:15181–15192
38. Koffie RM, Hashimoto T, Tai HC, Kay KR, Serrano-Pozo A, Joyner D, Hou S, Kopeikina KJ, Frosch MP, Lee VM, Holtzman DM, Hyman BT, Spires-Jones TL: Apolipoprotein E4 effects in Alzheimer's disease are mediated by synaptotoxic oligomeric amyloid-beta. Brain 2012, 135:2155–2168
39. Belinson H, Lev D, Masliah E, Michaelson DM: Activation of the amyloid cascade in apolipoprotein E4 transgenic mice induces lysosomal activation and neurodegeneration resulting in marked cognitive deficits. J Neurosci 2008, 28:4690–4701
40. Fuentealba RA, Liu Q, Zhang J, Kanekiyo T, Hu X, Lee JM, LaDu MJ, Bu G: Low-density lipoprotein receptor-related protein 1 (LRP1) mediates neuronal Abeta42 uptake and lysosomal trafficking. PLoS One 2010, 5:e11884
41. Zerbinatti CV, Wozniak DF, Cirrito J, Cam JA, Osaka H, Bales KR, Zhuo M, Paul SM, Holtzman DM, Bu G: Increased soluble amyloid-beta peptide and memory deficits in amyloid model mice overexpressing the low-density lipoprotein receptor-related protein. Proc Natl Acad Sci U S A 2004, 101:1075–1080
42. Basak JM, Verghese PB, Yoon H, Kim J, Holtzman DM: Low-density lipoprotein receptor represents an apolipoprotein E-independent pathway of Abeta uptake and degradation by astrocytes. J Biol Chem 2012, 287:13959–13971
43. Jiang Q, Lee CY, Mandrekar S, Wilkinson B, Cramer P, Zelcer N, Mann K, Lamb B, Willson TM, Collins JL, Richardson JC, Smith JD,

Comery TA, Riddell D, Holtzman DM, Tontonoz P, Landreth GE: ApoE promotes the proteolytic degradation of Abeta. Neuron 2008, 58: 681−693

44. Cramer PE, Cirrito JR, Wesson DW, Lee CY, Karlo JC, Zinn AE, Casali BT, Restivo JL, Goebel WD, James MJ, Brunden KR, Wilson DA, Landreth GE: ApoE-directed therapeutics rapidly clear beta-amyloid and reverse deficits in AD mouse models. Science 2012, 335:1503−1506
45. Saavedra L, Mohamed A, Ma V, Kar S, de Chaves EP: Internalization of beta-amyloid peptide by primary neurons in the absence of apolipoprotein E. J Biol Chem 2007, 282:35722−35732
46. Kandimalla KK, Scott OG, Fulzele S, Davidson MW, Poduslo JF: Mechanism of neuronal versus endothelial cell uptake of Alzheimer's disease amyloid beta protein. PLoS One 2009, 4:e4627
47. Lacor PN, Buniel MC, Furlow PW, Clemente AS, Velasco PT, Wood M, Viola KL, Klein WL: Abeta oligomer-induced aberrations in synapse composition, shape, and density provide a molecular basis for loss of connectivity in Alzheimer's disease. J Neurosci 2007, 27: 796−807
48. Shankar GM, Bloodgood BL, Townsend M, Walsh DM, Selkoe DJ, Sabatini BL: Natural oligomers of the Alzheimer amyloid-beta protein induce reversible synapse loss by modulating an NMDA-type glutamate receptor-dependent signaling pathway. J Neurosci 2007, 27: 2866−2875
49. Snyder EM, Nong Y, Almeida CG, Paul S, Moran T, Choi EY, Nairn AC, Salter MW, Lombroso PJ, Gouras GK, Greengard P: Regulation of NMDA receptor trafficking by amyloid-beta. Nat Neurosci 2005, 8:1051−1058
50. Perez-Otano I, Ehlers MD: Homeostatic plasticity and NMDA receptor trafficking. Trends Neurosci 2005, 28:229−238
51. Knobloch M, Konietzko U, Krebs DC, Nitsch RM: Intracellular Abeta and cognitive deficits precede beta-amyloid deposition in transgenic arcAbeta mice. Neurobiol Aging 2007, 28:1297−1306
52. Oddo S, Caccamo A, Shepherd JD, Murphy MP, Golde TE, Kayed R, Metherate R, Mattson MP, Akbari Y, LaFerla FM: Triple-transgenic model of Alzheimer's disease with plaques and tangles: intracellular Abeta and synaptic dysfunction. Neuron 2003, 39:409−421
53. Billings LM, Oddo S, Green KN, McGaugh JL, LaFerla FM: Intraneuronal Abeta causes the onset of early Alzheimer's disease-related cognitive deficits in transgenic mice. Neuron 2005, 45:675−688
54. Garcia-Alloza M, Robbins EM, Zhang-Nunes SX, Purcell SM, Betensky RA, Raju S, Prada C, Greenberg SM, Bacskai BJ, Frosch MP: Characterization of amyloid deposition in the APPswe/PS1dE9 mouse model of Alzheimer disease. Neurobiol Dis 2006, 24: 516−524
55. Holtzman DM, Fagan AM, Mackey B, Tenkova T, Sartorius L, Paul SM, Bales KR, Hsiao Ashe K, Irizarry MC, Hyman BT: Apolipoprotein E facilitates neuritic and cerebrovascular plaque formation in an Alzheimer's disease model. Ann Neurol 2000, 47:739−747
56. Bales KR, Liu F, Wu S, Lin S, Koger D, DeLong C, Hansen JC, Sullivan PM, Paul SM: Human APOE isoform-dependent effects on brain beta-amyloid levels in PDAPP transgenic mice. J Neurosci 2009, 29:6771−6779
57. Castellano JM, Kim J, Stewart FR, Jiang H, DeMattos RB, Patterson BW, Fagan AM, Morris JC, Mawuenyega KG, Cruchaga C, Goate AM, Bales KR, Paul SM, Bateman RJ, Holtzman DM: Human apoE isoforms differentially regulate brain amyloid-β peptide clearance. Sci Transl Med 2011, 3:89ra57
58. Tampellini D, Magrane J, Takahashi RH, Li F, Lin MT, Almeida CG, Gouras GK: Internalized antibodies to the Abeta domain of APP reduce neuronal Abeta and protect against synaptic alterations. J Biol Chem 2007, 282:18895−18906
59. DeMattos RB, Bales KR, Cummins DJ, Dodart JC, Paul SM, Holtzman DM: Peripheral anti-A beta antibody alters CNS and plasma A beta clearance and decreases brain A beta burden in a mouse model of Alzheimer's disease. Proc Natl Acad Sci U S A 2001, 98:8850−8855